

An Unusual Domino *Retro-Ene*–*Conia* Reaction: Regio- and Stereoselective One-Carbon Ring Expansion of Fenchol Derivatives

by Georg Ruedi*¹⁾, Dimitri N. Laikov, and Hans-Jürgen Hansen

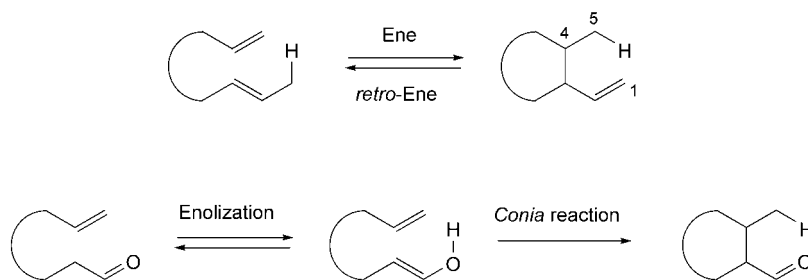
Organisch-chemisches Institut der Universität Zürich, Winterthurerstrasse 190, CH-8057 Zürich
(phone: +4116354248; fax: +4116356853; e-mail: georg@access.unizh.ch)

The 2-*exo*-substituted fenchol derivatives **1**–**7**, easily prepared from (–)-fenchone in good-to-excellent yields, were pyrolyzed by dynamic gas-phase thermo-isomerization (DGPTI). At temperatures of ca. 620°, the substrates with a hydroxyallyl (**1**–**4**) or a hydroxypropargyl moiety (**6**) underwent an initial *retro-ene* reaction under cleavage of the C(2)–C(3) bond to form enol-ene intermediates with no loss of optical activity. These intermediates then experience either tautomerization to the corresponding α,β -unsaturated ketones or subsequent *Conia* rearrangement under one-carbon ring expansion of the fenchone system to a bicyclo[3.2.1]octane framework. In the case of the isopropenyl substrate **3**, the sterically crowded *Conia* product underwent a new type of ‘deethanation’ reaction by stepwise loss of two Me radicals, giving rise to the thermodynamically favored enone **21**. A similar relaxation behavior was observed in the case of the ethynyl substrate **6**, which showed a remarkable 1,3-Me shift after the *Conia* reaction, leading to the α,β -unsaturated cyclic ketone **25**. The homolytic cleavage of the weakest single bond in **1**–**3** turned out to be a competing reaction pathway. Intramolecular H-abstraction within the generated diradical intermediates produced the monocyclic ketones **8**, **16**, and **19**, besides the products obtained by tautomerization and *Conia* reaction. In contrast, a Ph substituent at C(2) in **7** allowed only the passage through a diradical species to provide phenone **26**, which was converted by regioselective *Baeyer–Villiger* oxidation to the optically active cyclopentanol **29**. Both reaction channels, the domino *retro-ene*–*Conia* rearrangement and the diradical-promoted H-transfer, have been shown to proceed highly stereoselectively. The absolute configuration of the newly formed stereogenic centers in all compounds was assigned by ¹H-NOE experiments. The reaction mechanism of the novel domino *retro-ene*–*Conia* reaction was established by both a series of ²H- and ¹³C-labeling experiments, as well as by a detailed computational analysis.

1. Introduction. – The ene reaction is considered to be the transfer of a H-atom in allylic position from an ene donor to an ene acceptor with accompanying formation of a bond between these two moieties [1–4]. Formally, the ene reaction is a concerted $[2\pi_s + 2\pi_s + 2\sigma_s]$ process, thus allowing the stereospecific synthesis of optically active target molecules from chiral substrates. Intramolecular ene reactions are by far more favored energetically than their intermolecular counterparts due to entropic effects that lower the activation energy. Although alkynes appear to be more-reactive H-acceptors than olefins because of advantageous orbital overlap [5][6], their application is found far less frequently in the literature. Running the reaction in its reverse sense involves the thermal reversion of the above process. Such *retro-ene* reactions take place as intramolecular processes favored when raising the temperature, mainly for entropic reasons [6][7]. To prevent cleavage into two product molecules, C(4) or C(5) in the ene adduct must be bridged with the olefin part by a common ring system. As exemplified in *Scheme 1*, this so-called internal *retro-ene* reaction can be considered as a 1,5-H shift,

¹⁾ Part of the Ph.D. thesis of G. R., University of Zurich, 2004.

Scheme 1

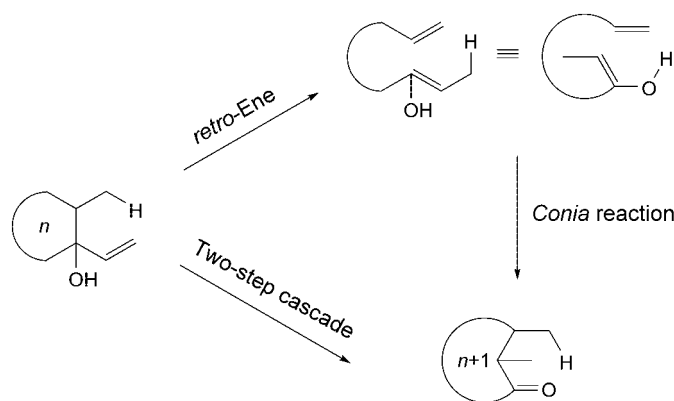


transforming a bicyclic substrate into an open-chain isomeric diene, which is accompanied by strain release [8]. In contrast to conventional *retro-ene* reactions, the equilibrium of internal *retro-ene* reactions lies completely on the side of the diene products.

Among the many hetero-ene reactions reported in the literature, the enol-ene reaction is well-recognized and broadly used as an effective tool in preparative organic synthesis. This concerted six-electron process, closely related to the parent ene reaction, has extensively been investigated by *Conia* and co-workers [9]. This so-called *Conia* reaction involves the thermal cyclization of ω -olefinic carbonyl compounds. An initial enolization step leads to the enol-ene substrate, and subsequent intramolecular ring closure leads to 1-cycloalkylalkanones. Due to the difference in thermodynamic stability between the carbonyl products and the enol substrates, a back reaction in terms of a *retro-Conia* process has not to be taken into account, when the formed ring possesses more than four ring atoms [4][8]. However, very few compounds including cyclopropyl and cyclobutyl ketones have been reported to undergo *retro-Conia* process [10]. In general, alkenes can be replaced by alkynes [3].

However, the enol-ene feature required for a *Conia* reaction can also be obtained, e.g., by a *retro-ene* reaction of 1-vinylcycloalkanols under ring opening (*Scheme 2*). This fragmentation/recyclization procedure would, thus, allow a formal one-carbon

Scheme 2



ring-expansion process, which has, to the best of our knowledge, not been reported in the literature so far. In continuation of our studies concerning the preparation of functionalized optically active compounds based on dynamic gas-phase thermo-isomerization (DGPTI), we describe herein the first examples of a domino *retro-ene*–*Conia* reaction and its application to the synthesis of synthetically versatile chiral building blocks.

2. Results and Discussion. – 2.1. *Synthesis of the 2-exo-Substituted Fenchol Substrates 1–7.* The CeCl_3 -mediated²⁾ addition of vinyl *Grignard* reagents to (–)-fenchone carried out in THF at ambient temperature afforded the tertiary *endo*-alcohols **1–3** in excellent yields (92–95%) and diastereoselectivities (*de* > 95%)³⁾, as shown in the *Table*. The minor amount of *exo*-isomer could easily be removed in each case by column chromatography. The high selectivity can be rationalized in terms of nucleophilic addition taking place preferentially from the *exo*-side of the $\text{C}=\text{O}$ face due to the steric hindrance of the *endo*-Me group at C(3). 2-Propenylfenchol (**2**) was obtained as a 1:1 mixture of (*E/Z*)-isomers, which could be separated by chromatography. The preparation of fenchol **4** under similar conditions with but-2-en-2-yl magnesium bromide could not be accomplished. Even at higher temperatures and with increasing amounts of CeCl_3 , only poor yields (< 10%) were obtained. Instead, the use of 2 equiv. of the corresponding organolithium reagent led to the desired product in

Table. CeCl_3 -Promoted Addition of Organometallic Reagents to (–)-Fenchone

R	Product	CeCl_3 [equiv.]	M	T [°]	Yield [%]
	1	0.8	MgBr	25	95
	(<i>E/Z</i>)- 2	0.8	MgBr	25	92
	3	0.8	MgBr	25	96
	(<i>E/Z</i>)- 4	1.1	Li	–20	43
	5	0.8	Li	–10	99
	7	–	Li	10	89

2) As reported by *Dimitrov et al.*, the use of stoichiometric amounts of CeCl_3 is essential to effect complete conversion [11].

3) Determined either by GC or NMR.

43% yield, when conducting the reaction at -20° . Although an isomeric mixture of (*E*)- and (*Z*)-but-2-en-2-yl lithium was allowed to react with the substrate, (*E*)-**4** was predominantly formed. The geometry of the trisubstituted C=C bond was established by 2D-NOE measurements at 600 MHz (CDCl_3). The $^1\text{H-NMR}$ spectrum of crude **4** indicated a minor amount of (*Z*)-**4** (15%). The preferential formation of (*E*)-**4** can be rationalized by faster attack of (*Z*)-(1-methylpropenyl)lithium relative to the corresponding (*E*)-analogue [12].

The *exo*-configuration of the 2-vinylfenchols **1–4** was ascertained by $^1\text{H-NOE}$ measurements (*Fig. 1*). The $^1\text{H-NMR}$ spectrum of **1** contained two signals for the H-atoms on the CH_2 bridge of the bicyclic terpene skeleton. As illustrated in *Fig. 1*, irradiation of the downfield *syn*-H-atom at $\delta(\text{H})$ 1.75 enhanced the resonance of the olefinic H-atom at $\delta(\text{H})$ 5.04, while irradiation of the upfield *anti*-H-atom at $\delta(\text{H})$ 1.18 produced NOE effects for both *exo*-H-atoms at C(5) and C(6), respectively. An NOE effect was further observed between the OH H-atom at $\delta(\text{H})$ 1.24 and H_{endo} -C(6) at 1.98. Compounds **2–4** exhibited comparable NOE interactions (*cf. Fig. 1*).

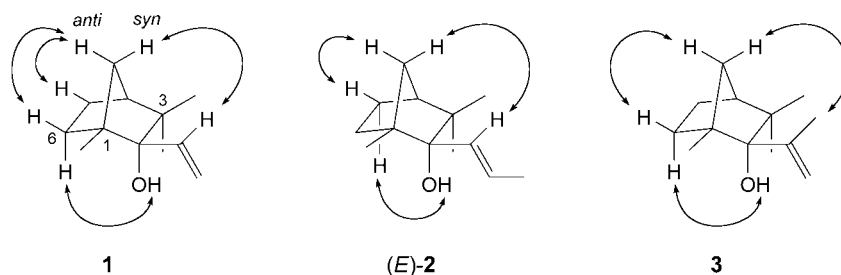
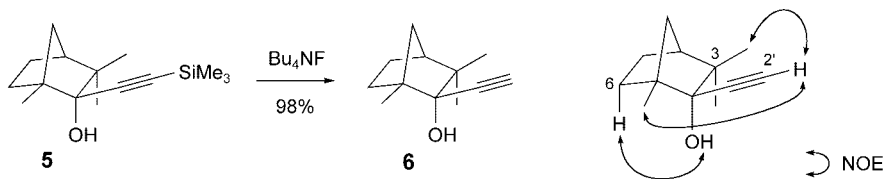


Fig. 1. Diagnostic $^1\text{H-NOE}$ correlations of β -fenchyl alcohols **1**, (*E*)-**2**, and **3**, all with *exo*-configurations

Fenchol derivatives with a 2-*exo*-ethynyl moiety such as **5** and its derivative **6** were synthesized similarly⁴⁾. The addition of lithium trimethylsilyl acetylide, freshly prepared by dropping BuLi to (trimethylsilyl)acetylene at -10° , to (–)-fenchone in the presence of 0.8 equiv. of CeCl_3 gave the propargylic alcohol **5** in almost quantitative yield (*Table*) [16]. Compound **5** was then smoothly deprotected to **6** by treatment with tetrabutylammonium fluoride (TBAF) in THF at -10° (98% yield of isolated material), as illustrated in *Scheme 3*. The alkyne signals gave rise to chemical shifts (CDCl_3) of $\delta(\text{C})$ 85.6 (*s*, C(1')) and 74.9 (*d*, C(2')), while the equivalent C-atoms in **5** were shifted downfield to $\delta(\text{C})$ 107.8 (*s*, C(2')) and 91.1 (*s*, C(1')), being more separated ($\Delta\delta$ *ca.* 17 ppm). On the other hand, C(2) in **5** and **6** resonated at almost the same frequency (80.9 and 80.6 ppm, respectively). Furthermore, both **5** and **6** exhibited a characteristic band in their IR spectra at 2164 and 2104 cm^{-1} , respectively, for their triple bond. In contrast to the 2-*exo*-vinyl alcohols **1–4**, having all negative $[\alpha]_{\text{D}}$ values, the optical rotations of **5** and **6** exhibited positive values (+17.2 and +19.6, respectively). Establishing the spatial structure of **5** turned out to be rather delicate due to the linearity of the ethynyl group. As shown in *Scheme 3*, complete assignment could be achieved by irradiating the OH H-atom at $\delta(\text{H})$ 1.83, which caused an NOE

⁴⁾ Interestingly, the class of 2-ethynyl-substituted fenchol derivatives has been sparsely investigated [13–15].

Scheme 3



effect for $H_{endo}-C(6)$ at 1.67 ppm. Irradiation of the signal of the acetylenic H-atom at $\delta(H)$ 2.55 enhanced both the bridgehead Me resonance at 1.20 and the *exo*-Me resonance at 1.12 ppm.

Although the *exo*-trajectory of nucleophilic attack to (–)-fenchone is well-established, the $CeCl_3$ -promoted addition of $PhMgBr$ to (–)-fenchone in THF, as reported by *Dimitrov et al.* [11], afforded 2-phenylfenchol (**7**) only as a 1:1 mixture of the *endo*- and *exo*-isomers, which was evident from 1H - and ^{13}C -NMR analyses. The following modifications had to be made to improve the diastereoisomeric ratio: 1) carrying out the transformation in a nonpolar solvent [17][18] (in our case, the reaction was performed in a 2:2:1 mixture of Et_2O , toluene, and hexane); 2) using a freshly prepared $PhLi$ solution instead of the corresponding *Grignard* reagent; 3) inverse addition at low temperature (10°), *i.e.*, dropwise addition of (–)-fenchone to a vigorously stirred solution of the nucleophile; and 4) absence of *Lewis* acids to prevent the nucleophile from adding too fast (unselectively) to the $C=O$ group. These modifications allowed selective addition to the sterically less-hindered *exo*-face of the bicyclic ketone under formation of (–)-*exo*-2-phenylfenchol (**7**; 89%). Its spectroscopic and physical data were identical in all respects with those reported in [19].

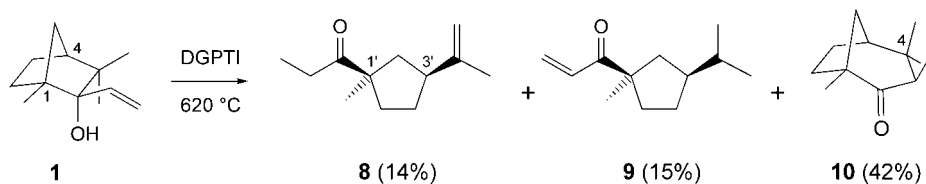
2.2. Dynamic Gas-Phase Thermo-Isomerizations. All thermal transformations were carried out in a flow-reactor system under vacuum conditions ($2-4 \times 10^{-2}$ mbar) by evaporating the fenchol substrates through a quartz tube (100-cm length, 3 cm i.d.) preheated by a tube furnace (the estimated residence time of the molecules in the reactor is in the range of milliseconds). A flow of carrier gas (N_2) was applied to keep a constant flow along the tube. The rearranged material was then trapped at low temperature immediately after passing the hot zone (for details, see [20–22] and the *Exper. Part*).

2.2.1. Isomerization of 2-Vinylfenchols 1–4. We started our investigations with the 2-vinyl derivative **1**. Studies on the influence of the reaction temperature on the thermal isomerization revealed optimal conversion at 620° in combination with a flow rate of 1.0 l/h⁵). Preliminary data on the rearrangement products of **1** indicated the presence of the three isomeric compounds **8–10** (m/z 180) in a 1:1:3 ratio⁶) (*Scheme 4*). After chromatographic separation, the structural features of the two minor components were established by NMR spectroscopy. The 1H -NMR spectrum of **8** showed the signals of two olefinic H-atoms, each appearing as a broad *singlet* at $\delta(H)$ 4.65 and 4.62, as well as

⁵) The optimal conditions for DGPTI of each substrate were established by a series of test runs monitored by GC/MS. Thereby, the reactor temperature as well as the flow rate were systematically altered.

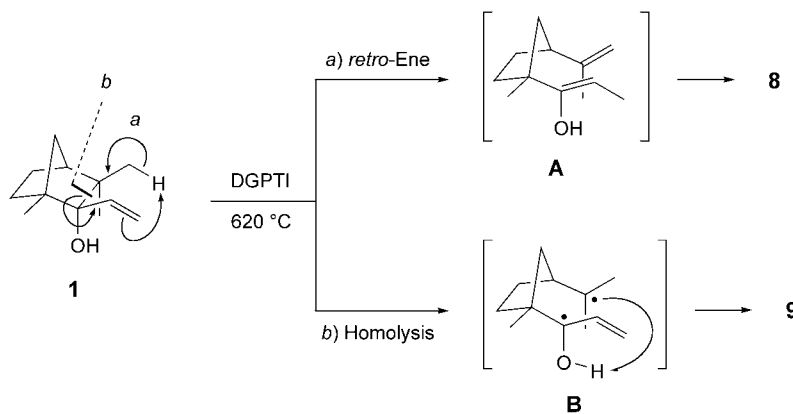
⁶) Determined by GC/MS analysis.

Scheme 4



the feature of an ethyl ketone. The ^{13}C -NMR spectrum exhibited a set of characteristic absorptions at $\delta(\text{C})$ 146.6, 107.8, and 20.0, respectively, consistent with an isopropenyl (=1-methylethenyl) group. These data are in agreement with 1-(3-isopropenyl-1-methylcyclopentyl)propan-1-one (**8**), presumably formed *via* a *retro-ene* reaction involving the *exo*-Me group at C(3) under cleavage of the C(2)–C(3) bond. This course of events contrasts in a striking way to that observed in the camphor series [23][24]. According to *Scheme 5*, the initially formed enol intermediate **A** might survive only in the gas phase, and tautomerization to ketone **8** would occur only in the condensed phase (cooling trap) as an intermolecular process. Assuming the stereogenic centers at C(1) and C(4) are not involved in the rearrangement, the entire stereochemical information had been transferred with no loss of optical activity. This finding was further supported by ^1H -NOE experiments, showing strong interactions between H–C(3') (*m*) and Me–C(1') (*s*), thus indicating that both substituents are located at the 'endo-face' of the cyclopentane ring. Further significant NOEs were observed between $\text{CH}_2(2)$ and both *exo*-H–C(2') and *exo*-H–C(5'). The ^1H -NMR spectrum of **9** showed characteristic downfield-shifted signals of an *ABX* system belonging to a terminal vinyl group next to a C=O function. Furthermore, there was no evidence for an isopropenyl group. Apart from that, the spectral data of **9** were almost identical to those recorded for **8**. Moreover, the $[\alpha]_{\text{D}}$ values of both compounds (-8.9 and -6.2 , resp.) indicated a very close structural relationship. These observations are in accordance with the proposed structure of propenone **9**. It is further noteworthy that the formation of **8** and **9** occurred with no loss of optical activity.

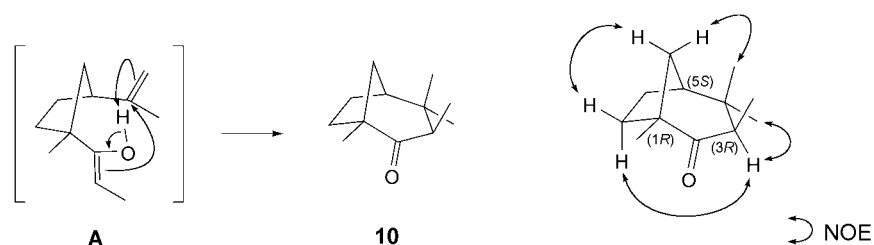
Scheme 5



The formation of **9** involves the homolytic cleavage of the C(2)–C(3) bond in **1** under formation of a hydroxyallyl tertiary-alkyl diradical **B** and subsequent stereoselective intramolecular H-abstraction from the OH group (*Scheme 5*). Similar disproportionation reactions had recently been observed in our group, when phenylisoborneols⁷⁾ [23][24] or macrocyclic 1-phenylcycloalkanols [25] were thermo-isomerized under similar conditions. The diradical-promoted formation of **9** is even more striking, since the related thermal isomerization of vinylisoborneol has been found to proceed exclusively through a concerted *retro-ene* reaction [24].

Surprisingly, the NMR data of the major component **10** provided no evidence for an olefin. Furthermore, its $[\alpha]_D$ value (-42.8) significantly deviated from those of **8** and **9**. These observations strongly pointed at a fundamentally different framework. Eventually, the structure of **10** was elucidated by in-depth spectroscopic investigations, revealing a bicyclo[3.2.1]octan-2-one skeleton⁸⁾. As shown in *Scheme 6*, the structural features of the enol intermediate **A** allow a subsequent *Conia* reaction. In this specific case, the *Conia* reaction occurred under expansion of the bicyclic fenchone skeleton by one C-atom, leading to the 3-methylhomofenchone **10**.

Scheme 6



The full three-dimensional structure of **10** was investigated by ¹H-NOE experiments, showing the configuration at C(3) to be (*R*), with an *exo*-Me group. The absolute configuration at C(3) could not be directly confirmed, but can be assigned on the basis of the known absolute configurations at C(1) and C(4) in **1**, assuming that these stereogenic centers⁹⁾ were not involved in a bond-breaking process. From these observations, it is evident that the *Conia* reaction proceeds stereoselectively *via* intermediate **A**.

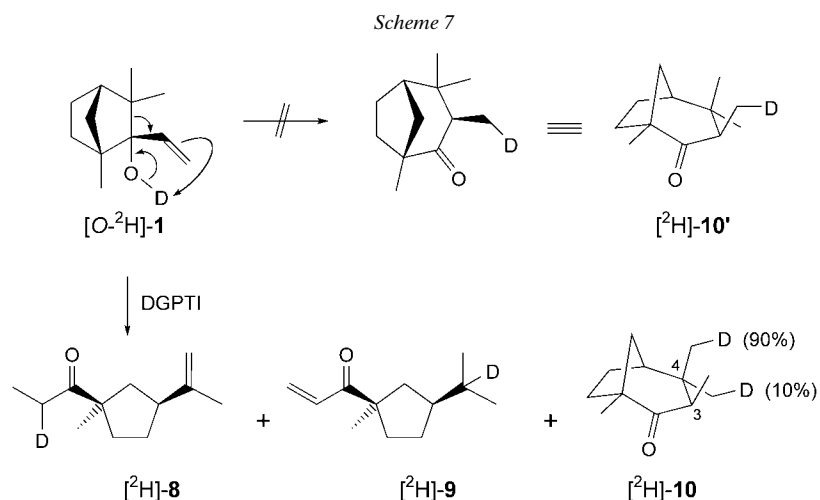
In order to more amply investigate the stereochemical course of this remarkably selective *retro-ene*–*Conia* sequence, we prepared the *O*-deuterated fenchol [*O*-²H]-**1** by repeated treatment of **1** with MeOD and D₂O¹⁰⁾. Thermo-isomerization as above

7) In remarkable contrast, we have found that phenylisoborneols undergo clean homolysis of the C(1)–C(2) bond under formation of a diradical intermediate involving a tertiary radical at the former bridgehead position.

8) A similar one-carbon ring expansion leading to the same skeleton was reported by *Paquette et al.* [26]. Acid-catalyzed isomerization of dihydrofurylfenchol with TsOH provided in a *Wagner–Meerwein* rearrangement dihydrospirobicyclo[3.2.1]octanone. However, the acidic conditions gave rise to the formation of all possible regio- and stereoisomers.

9) C(1) and C(4) in **1** correspond to C(1) and C(5), respectively, in **10**.

10) The deuterium content was determined by GC/MS.



provided the respective deuterated compounds $[^2H]-8$, -9 , and -10 , which were purified chromatographically and analyzed by 2H -NMR spectroscopy (Scheme 7). The label in $[^2H]-8$ was found at $\delta(D)$ 2.44 as a broad *singlet*, while $[^2H]-9$ exhibited a *singlet* at $\delta(D)$ 1.25. In the case of $[^2H]-10$, the label had been introduced into the *exo*-Me group at C(4), appearing as a broad *singlet* at $\delta(D)$ 0.98. Interestingly, a minor absorption, accounting for *ca.* 10% of the 2H content in $[^2H]-10$, was observed at $\delta(D)$ 0.69 (*endo*-Me group at C(4)), which might be due to the free rotation of the isopropenyl group about its single bond in intermediate **A**.

These results strengthen the hypothesis of a *retro*-ene – *Conia* cascade in two steps. Furthermore, the labeling experiment showed that no D-atom was found at the *exo*-Me group at C(3), as would be present in $[^2H]-10'$ (Scheme 7). Thus, an alternative reaction pathway that would yield **10** directly from **1** in only one step via *Wagner–Meerwein* rearrangement [27] can definitively be ruled out.

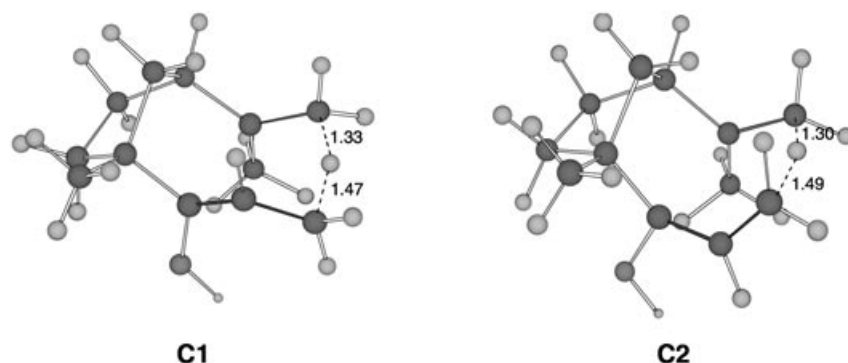
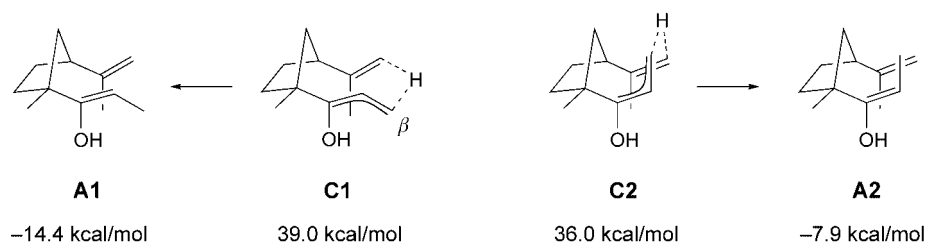
To get further information on the mechanism of this highly stereoselective reaction sequence and to rationalize the formation of minor side products that could well have been formed but were not detected spectroscopically, we performed a detailed computational analysis¹¹), as structurally outlined in Scheme 8. Examination of DFT-calculated¹²) transition-state models for the *retro*-ene reaction reveals that there are generally two possible arrangements **C1** and **C2** with either (*Z*)- or (*E*)-configuration of the involved hydroxyallyl system¹³). Following this analysis, transition state **C1** would lead to the thermodynamically favored (*Z*)-enol intermediate **A1**, whereas **C2** would lead to the (*E*)-enol intermediate **A2** by surmounting an energy barrier somewhat lower than the alternative one depicted in **C1** ($\Delta\Delta G_{393}^\ddagger = 3.0$ kcal mol⁻¹).

¹¹) PBE Density-functional theory [28] has been implemented in the computer program written by Laikov [29]. Full geometry optimizations for energy minima and transition states were followed by harmonic vibrational analysis to derive the thermochemical data.

¹²) Computed at 620° (893 K).

¹³) All relative energy values refer to substrate **1** (=0.0 kcal mol⁻¹).

Scheme 8

Fig. 2. Chem3D Structures of DFT-calculated transition states **C1** and **C2**

Global minimum-energy conformations of the two possible transition states **C1** and **C2** are displayed in Fig. 2. The interatomic distances between the transferred H-atom and the β -C-atom of the hydroxyallyl moiety of both **C1** and **C2** are similar, amounting to 1.47 and 1.49 Å, respectively. On the other hand, the interatomic distances between this particular H-atom and the C-atom at which this H-atom had formerly been bonded are significantly smaller, 1.33 and 1.30 Å, respectively, accounting for a 'reactant-character' of the transition states **C1** and **C2**.

Further DFT-calculated transition-state models for the subsequent *Conia* reaction showed four configurations to be compatible with this mechanism (Scheme 9, Fig. 3). Intermediate **A1**, containing a (*Z*)-C=C bond, allows two different transition states **D1** and **D2**. The former shows *endo*-arrangement of both participating π -systems, while an *exo*-arrangement is found in **D2**.

The relative energies after minimization of these transition-state models were compared. The results indicate that **D1**, leading to **10** with an *exo*-Me group at C(3), is marginally more stable (1.7 kcal mol⁻¹) than its competitor **D2**, which would lead to **11** with an *endo*-Me group at C(3). Since the difference between the calculated ΔG_{893} values for **10** and its epimer **11** was calculated to be 3.0 kcal mol⁻¹ in favor of **10**, any attempt to at least partially epimerize **10** at C(3), thus providing **11**, failed. On the other hand, both **10** and **11** would also be accessible *via* transition states **D3** and **D4**, both of

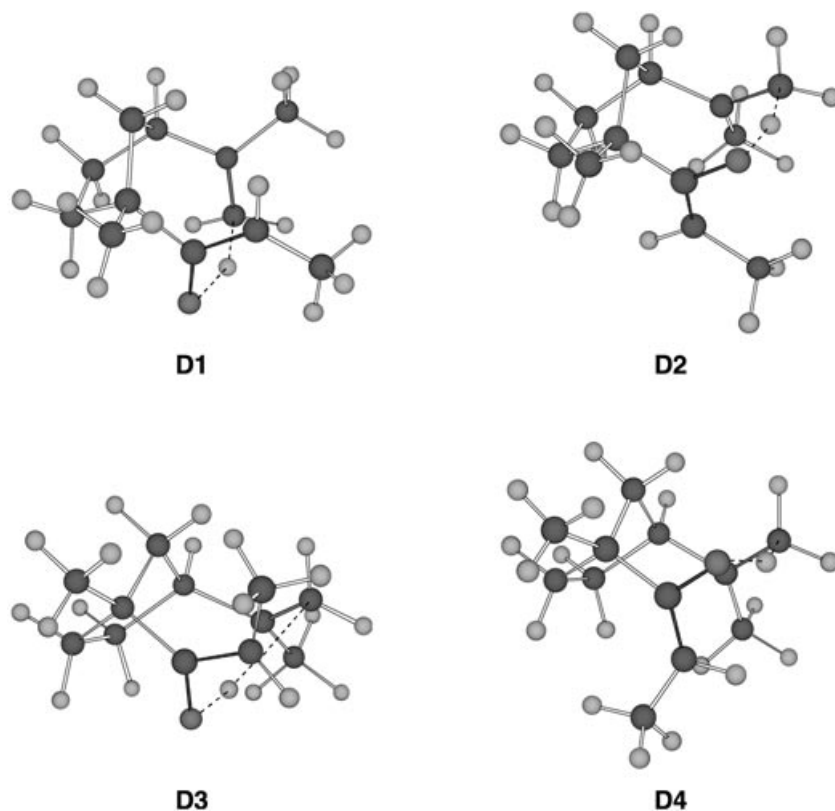


Fig. 3. Chem3D Structures of DFT-calculated transition states **D1**–**D4**

difficult. Since the ring enlargement of bicyclic systems is accompanied by strain release appreciably in excess of that encountered in going from more-conventional five- to six-membered rings, the sensitivity of **1** to DGPTI-promoted interconversion is entirely comprehensible.

Up to this point, we have only considered the *exo*-Me group at C(3) in substrate **1** to be an appropriate H-source for the initial *retro*-ene reaction. In the following, we will discuss whether there are further groups capable of undergoing such a process that have to be taken into account. The *endo*-Me H-atoms of the geminal dimethyl groups at C(3), however, are unable to interact with the C=C bond for geometric reasons, *i.e.*, the proximity of the groups involved cannot be achieved (4.07 Å¹⁶). On the other hand, a *retro*-ene reaction involving the bridgehead Me group, as we have found to occur as a side reaction when 2-vinylisoborneol was thermo-isomerized [24], would generally be feasible. As depicted in *Scheme 10*, transition state **E** would, thus, lead to enol intermediate **F**, which would give the monocyclic *exo*-methylidene compound **12** by tautomerization in the condensed phase, or the ring-expanded bicyclic ketone **13** via

¹⁶⁾ In contrast, the corresponding distance between the nearest *exo*-Me H-atom at C(3) and the vinyl moiety was calculated as 3.15 Å.

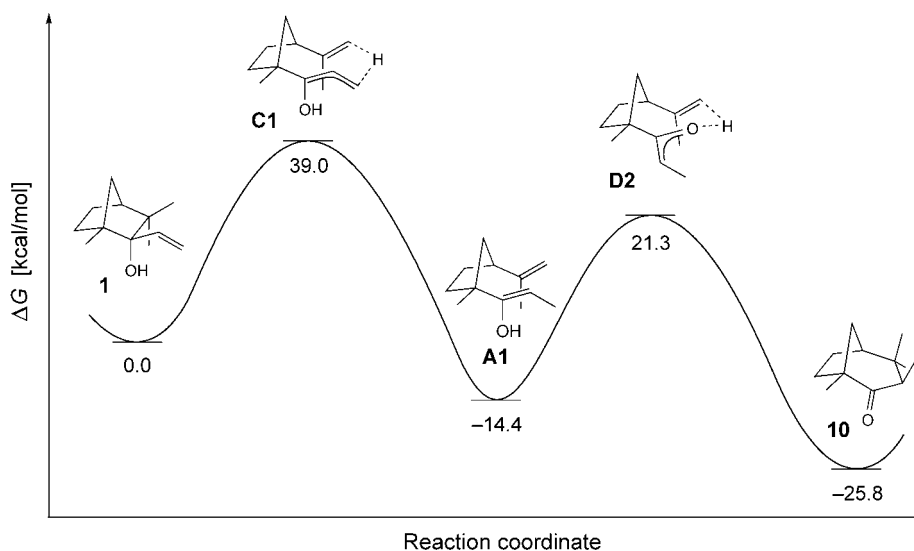
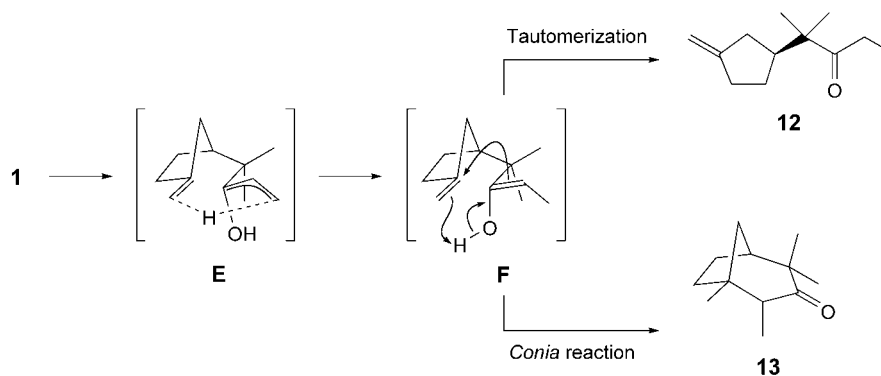


Fig. 4. Energy profile for the conversion of **1** to **10** via different transition states

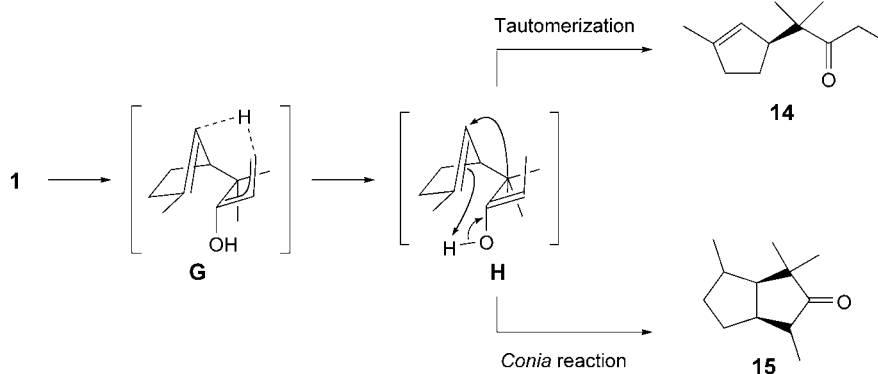
Scheme 10



Conia reaction. However, DFT-calculations showed that the activation barrier of the hypothetical transition state **E** is ca. 45 kcal mol⁻¹. Thus, **E** cannot efficiently compete with **C1**.

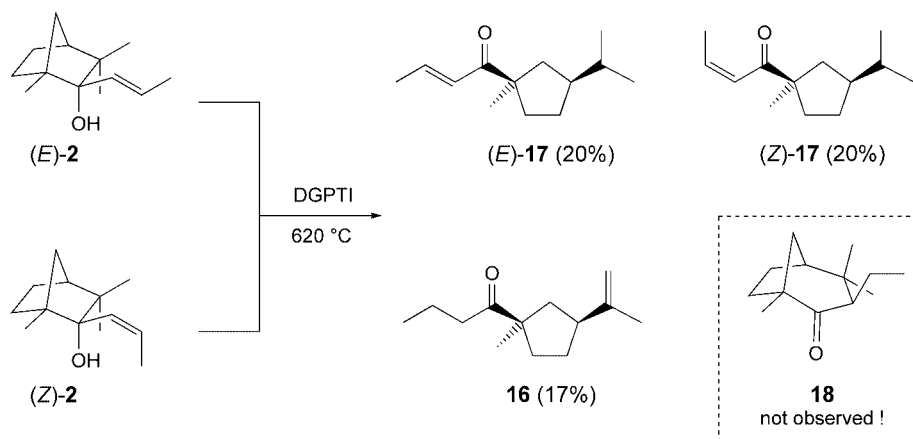
Alternatively, another *retro-ene* process in this system might also pass through the hypothetical transition state **G** (Scheme 11). In this particular case, the vinyl moiety is directed to the bridge to adequately interact with H_{syn}, thus providing enol **H**. Keto/enol tautomerization would then lead to **14** with an endocyclic C=C bond. Likewise, intermediate **H** could undergo *Conia* reaction in the usual manner, giving *cis*-connected hexahydropentalenone **15**. However, this route violates *Bredt's* rule in the first step [30]. Therefore, a *retro-ene* reaction via **G** must overcome an energy barrier significantly higher than the alternative modes mentioned above.

Scheme 11



In contrast to **1**, thermal isomerization of (*E/Z*)-1,3,3-trimethyl-2-*exo*-propenylbicyclo[2.2.1]heptan-2-ol (**2**)¹⁷ at 620° afforded only the monocyclic ethylketone **16** (17%) via a *retro*-ene process, together with a 1:1 mixture of (*E/Z*)-**17** (40%)¹⁸ formed by diradical-mediated intramolecular disproportionation by H-transfer, in analogy to the formation of **9** (Scheme 12). This product mixture was accompanied by a variety of low-boiling side products (*ca.* 35%), which were not further characterized. Lower reaction temperatures provided smaller amounts of side products, but an increasing amount of unreacted starting material¹⁹). It is further interesting to state that the pure isomers (*E*)- and (*Z*)-**2**, respectively, gave rise to the same product mixture. Apparently, (*E*)/(*Z*)-isomerization occurred at the diradical stage to give a

Scheme 12



¹⁷⁾ 1:1-Mixture.

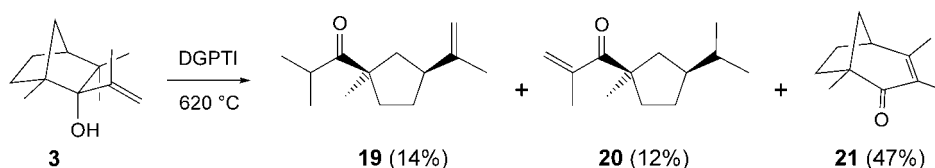
¹⁸⁾ Only (*E*)-**17** could be isolated in its pure form (20%). (*Z*)-**17** and **16** were obtained only as a mixture that could not further be purified.

¹⁹⁾ Starting material could be recovered only at reactor temperatures below 550°.

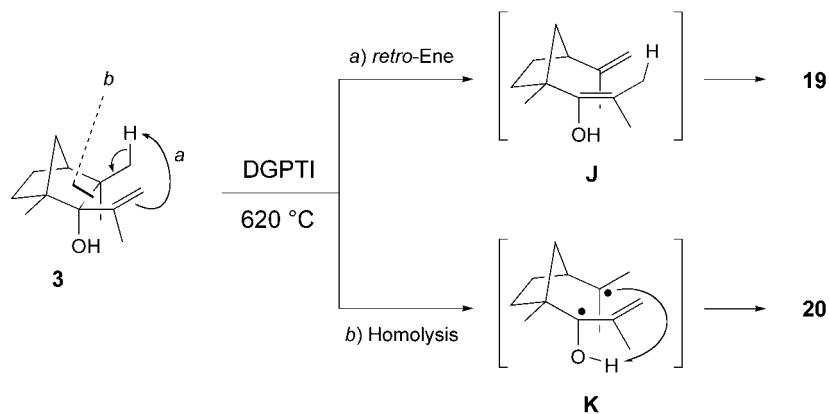
1:1 mixture of (*E/Z*)-**17**. The spectroscopic data indicated no evidence for a bicyclo[3.2.1]octan-2-one skeleton **18** with an *exo*-Et group at C(3), as would be expected in analogy to the pyrolysis of substrate **1**. Although initial *retro*-ene reaction leading to **16** was observed, the *Conia* rearrangement did not take place for reasons that we do not understand at the moment.

The key question emerging from the above findings was: what structural features are required for a specific fenchol substrate to undergo *Conia* reaction from an enolene stage primarily formed *via* a *retro*-ene process? To answer this question, we investigated the thermal behavior of the isomeric 2-*exo*-isopropenyl-substituted compound **3** (Scheme 13). Isomerization of **3** at 620 °C provided the three main products **19**, **20**, and **21** in a 1:1:4 ratio. Two minor components (<10%) were also present in the mixture, but could not be obtained in pure form by column chromatography. The spectral data of the pure compounds **19** (14%) and **20** (12%) were very similar to those recorded for propanone **8** and vinylketone **9**, respectively. The ¹H-NMR spectrum of **19** contained two broad *singlets* at δ (H) 4.72 and 4.69, the latter exhibiting a NOE effect with the *singlet* of the Me group at δ (H) 1.72, indicating an isopropenyl moiety. A downfield-shifted *septet* at δ (H) 3.03 ($J=6.7$ Hz) indicated an isopropyl ketone substructure. These data are in agreement with the structure of 2-methylpropanone **19** formed in a *retro*-ene reaction, followed by tautomerization of the intermediate enol **J** (Scheme 14). In contrast, the ¹H-NMR spectrum of **20** showed two broad *singlets* at δ (H) 5.64 and 5.60, indicating an isopropenyl group as part of an α,β -unsaturated system. A reaction mechanism involving the diradical intermediate **K**, followed by intramolecular H-transfer, would be consistent with these observations.

Scheme 13



Scheme 14



To our surprise, the GC/MS spectrum of the major component **21** (47%) showed an M^+ peak at m/z 164 instead of m/z 194, as would be expected for an isomeric compound. There are two explanations for this finding: 1) **21** is an isomeric product with m/z 194, but losing formally C_2H_6 (m/z 30) under the ionization conditions, or 2) a fragment of m/z 30 had been lost during DGPTI. This question was answered by recording a CI mass spectrum, revealing again a molecular peak at m/z 164. Thus, the DGPTI-promoted formation of **21** involves the loss of C_2H_6 .

As observed in the case of **10** (*vide supra*), **21** exhibited an $[\alpha]_D$ value (-110.9) that largely diverged from those of **19** (-6.1) and **20** (-5.8). Further clarification could be obtained with the aid of ^{13}C -NMR spectroscopy. The spectrum contained three characteristic signals, all appearing as *singlets* at $\delta(C)$ 204.0, 168.8, and 127.5. Such a pattern of a slightly downfield-shifted C=O group and a significantly downfield-shifted β -C-atom, reaching a value of nearly 170 ppm, would conform to an α,β -unsaturated ketone. In addition, three Me *singlets* appeared at $\delta(H)$ 1.96, 1.69, and 1.25. The chemical shifts of the first two signals are compatible with allylic Me groups, and the signal at $\delta(H)$ 1.25 corresponds to a Me group at a quaternary C-atom next to an electron-withdrawing functionality. According to Fig. 5, only the signal at $\delta(H)$ 1.96 exhibited a diagnostically relevant NOE effect. The 2D-NOE spectrum of **21** showed a cross-peak with a broad *triplet* at $\delta(H)$ 2.68. From these observations, we established the structure of **21** as 1,3,4-trimethylbicyclo[3.2.1]oct-3-en-2-one.

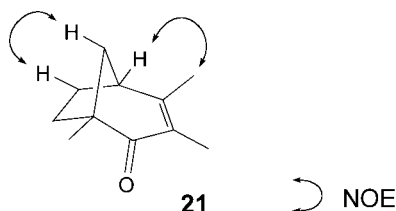
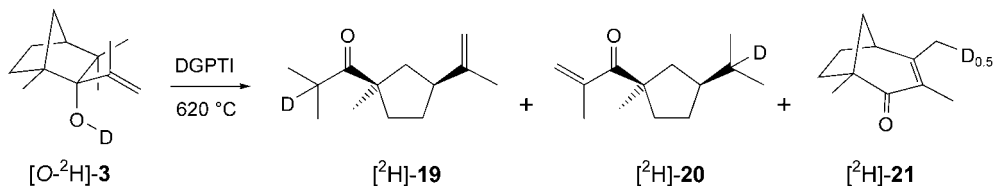


Fig. 5. Diagnostic 1H -NOE correlations of **21**

To gain insight into the pathway that led to **19–21**, a 2H -labeling study was performed with *O*-deuterated fenchol, [O - 2H]-**3**, prepared by H/D exchange (*vide supra*). As displayed in Scheme 15, pyrolysis of [O - 2H]-**3** afforded labeled **19–21** in almost the same ratio and yields as observed in the unlabeled cases. The 2H -NMR spectrum ($CDCl_3$) of [2H]-**19** showed a signal at $\delta(D)$ 3.04, corresponding to H–C(2) in the unlabeled analogue **19**. In [2H]-**20**, the label was found at $\delta(D)$ 1.23, indicating a methine C–H. In the case of deuterated **21**, the label had been introduced exclusively into the Me group at C(4), appearing as a broad *singlet* at $\delta(D)$ 1.96. However, interestingly, the 1H -NMR spectrum ($CDCl_3$) of [2H]-**21** indicated that the 2H content at C(4) was only 50%²⁰).

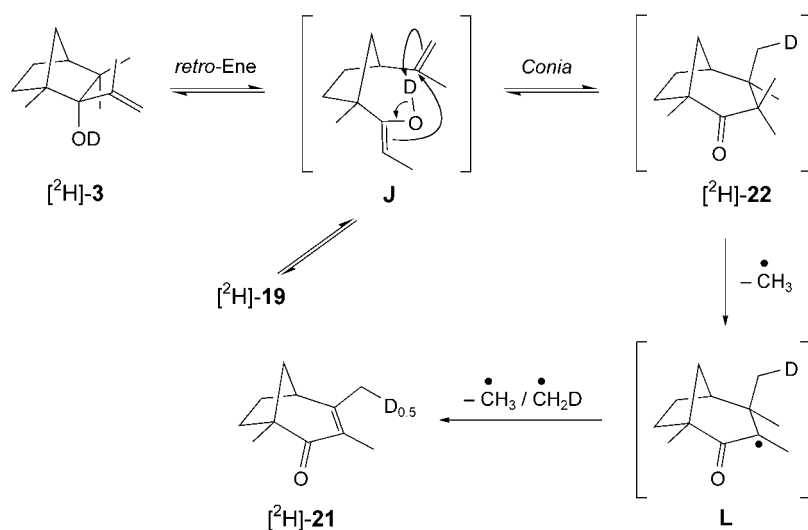
²⁰) In comparison with the Me group at C(3), corresponding to three H-atoms, the integral of the CH_2D group at C(4) indicated 2.5 H-atoms instead of the expected two H-atoms.

Scheme 15



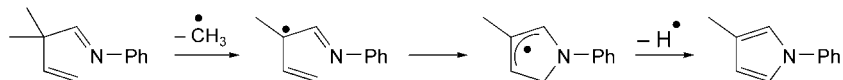
A plausible reaction pathway for the formation of $[^2H]-21$ is presented in Scheme 16. In analogy to substrate **1**, initial DGPTI-promoted *retro-ene* reaction provides the enol-ene intermediate **J**, which undergoes a *Conia* reaction under C_1 ring expansion. However, surprisingly, the spectroscopic data provided no evidence for the expected sterically congested bicyclic ketone $[^2H]-22$, exhibiting geminal dimethyl groups at both C(3) and C(4). However, taking into account the reactor temperature of 620° as well as the strain of this molecule, stepwise demethylation reactions may occur²¹).

Scheme 16



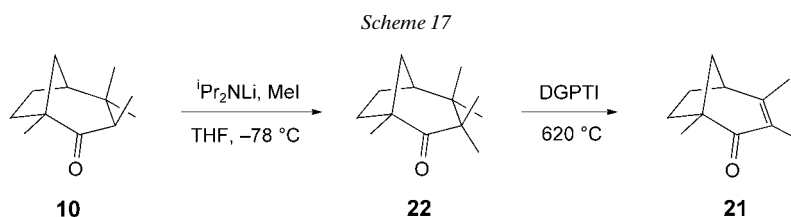
As we have reported recently, the activation energy of a specific homolytic processes can be approximated by the dissociation energy of the single bond to be broken [32–34]. The first demethylation step in Scheme 16, occurring at C(3) under formation of a stable tertiary acyloyl radical intermediate **L**, is assumed to have an

²¹) A similar demethylation reaction has earlier been observed when 2,2-dimethylbut-3-enylidene(phenyl)-amine was submitted to flash vacuum pyrolysis at 500° . The generated azapentadienyl radical underwent an electrocyclization and loss of a H-atom to give the observed pyrrole [31].

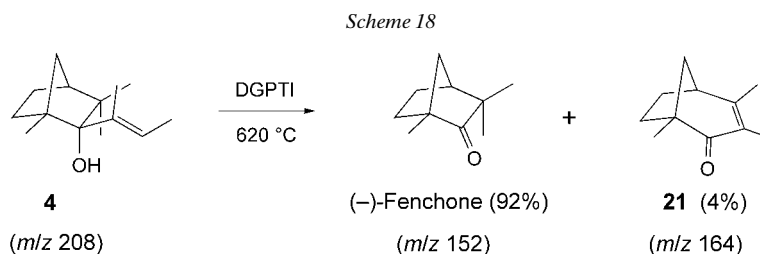


activation barrier of *ca.* 65 kcal mol⁻¹, which may easily be surmounted under the conditions applied. In addition, a Me-radical extrusion within the sterically overcrowded pentamethyl system [²H]-**22** is driven by strain release. Moreover, the susceptibility of the generated radical intermediate **L** to lose a further CH₃ or CH₂D radical under DGPTI conditions is perspicuous. As the deuterium content in [²H]-**21** was only 50%, the second demethylation step is assumed to occur with no selectivity.

As a control experiment, we independently synthesized the postulated intermediate **22** by α -methylation of **10** (Scheme 17). This was achieved by deprotonation at -78° , using a threefold excess of LDA ((i-Pr)₂NLi), followed by addition of an eightfold excess of MeI at the same temperature, to give **22** in 95% yield [35]. Indeed, submitting **22** to DGPTI at 620° yielded **21** as the main product²².



Increasing the steric hindrance on the vinyl moiety of the fenchol substrate by introducing an additional Me group dramatically affected the course of the DGPTI process (Scheme 18). According to GC/MS analysis, pyrolysis of **4** at 620° occurred very cleanly²³) to give two products in a 23:1 ratio. Surprisingly, both exhibited a molecular mass that was not compatible with an isomerization reaction. The major component showed a peak at *m/z* 152 instead of the expected *m/z* 208. The fragmentation patterns as well as the GC/MS retention times were identical with those for (–)-fenchone (92%). Apparently, cleavage to but-2-ene and (–)-fenchone is favored over both the homolysis of the C(2)–C(3) bond and the *retro*-ene reaction. Similar ‘*retro-Grignard*’ reactions had earlier been observed, when sterically crowded tertiary alcohols were exposed to high temperatures [36–39]. The minor component (4%) was shown to be trimethylbicyclo[3.2.1]oct-3-en-2-one (**21**) by co-injection with an authentic sample obtained by DGPTI of **3**. Amazingly, DGPTI of the two different

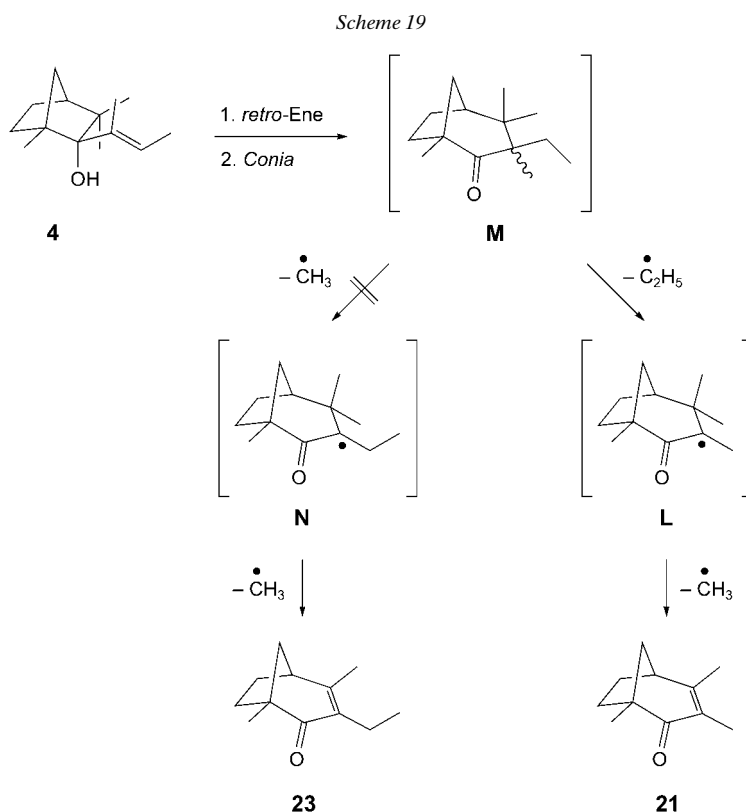


²²) A broad variety of low-boiling side products, accounting for *ca.* 30% of the product mixture, were also detected by GC/MS.

²³) Only a few unidentified products (<4%) were observed by GC/MS.

substrates **3** and **4** gave rise to a common product with a molecular mass differing from both substrates.

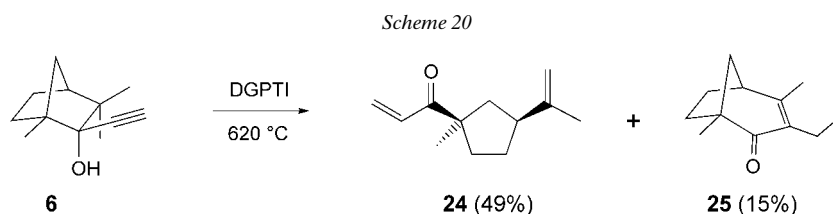
The formation of **21** can basically be described by two independent reaction mechanisms. In comparison with the pathway elaborated above, an alternative route, involving **4** as starting material, is depicted in *Scheme 19*. A domino *retro-ene*–*Conia* sequence would lead to a thermally unstable, ring-expanded intermediate **M** corresponding to **22** in the case of substrate **3**. Although **M** seems to be more stable than its pentamethyl analogue in terms of steric hindrance, homolytic cleavage under generation of a radical intermediate may occur. Extrusion of a Me radical would lead to **23** via intermediate **N**. But, as the Et radical is stabilized by hyperconjugation, passage through **L** and concomitant formation of **21** is presumed to be favored²⁴). However, GC/MS analysis provided no evidence for α -ethyl ketone **23** (m/z 178).



2.2.2. *Isomerization of 2-Ethynylfenchols 5 and 6*. We further extended our studies by replacing the 1-alkenyl group by an ethynyl functionality. According to *Scheme 20*, DGPTI of **6** afforded the two isomeric products **24** and **25** in a 3:1 ratio. Following chromatographic separation, the structural features of both compounds were eluci-

²⁴) The difference in radical-stabilization energies between a Me and an Et radical was determined to be *ca.* 5 kcal mol⁻¹.

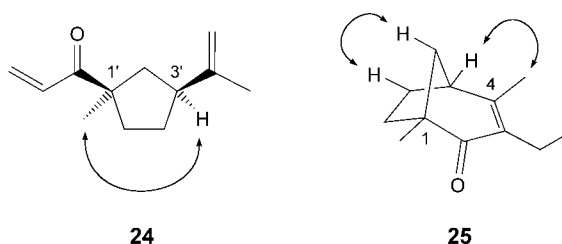
dated by NMR. The ^{13}C -NMR spectrum of the component first eluted contained four olefinic signals and one $\text{C}=\text{O}$ absorption at $\delta(\text{C})$ 202.7, and the ^1H -NMR spectrum showed a characteristic downfield-shifted ABX system, compatible with a vinyl ketone. In addition, two isolated *singlets* at $\delta(\text{H})$ 4.72 and 4.70 pointed to an isopropenyl group, as observed, *e.g.*, in the case of **8**. Moreover, an $[\alpha]_{\text{D}}$ value of -6.6 indicated that **24** and **8** were closely related. These findings are consistent with a product formed *via* a *retro-ene* process.



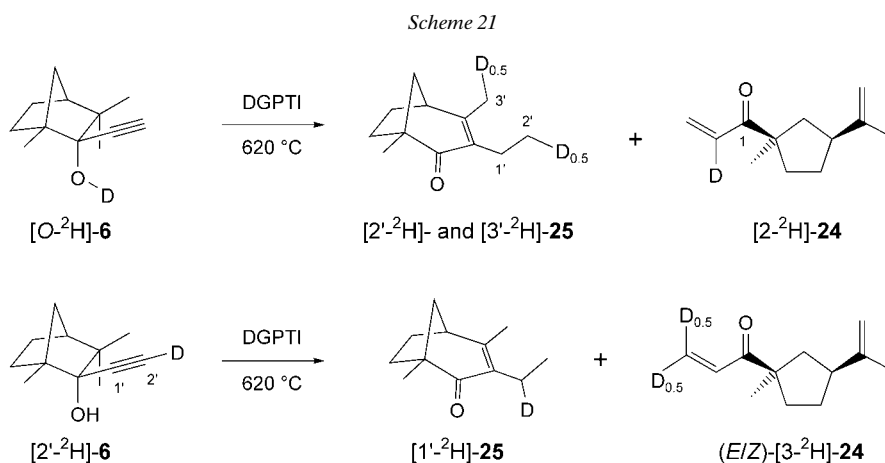
The ^1H -NMR spectrum of the minor component **25** contained only aliphatic signals; there was no evidence for an olefin at first sight. Interestingly, signals of an ABX_3 system, with $J_{AB} = 15.0$ Hz, appeared at $\delta(\text{H})$ 2.22 and 2.20, which indicated the presence of diastereotopic H-atoms of a CH_2 group linked to a Me group with $J_{AX} = J_{BX} = 7.5$ Hz. Of the two Me *singlets* at $\delta(\text{H})$ 1.96 and 1.24, the chemical shift of the former appeared to be characteristic for a Me group connected to an olefinic moiety. Otherwise, two downfield-shifted quaternary signals appeared at $\delta(\text{C})$ 160.3 and 133.6, which – in combination with a $\text{C}=\text{O}$ *singlet* at 203.4 ppm – seem to be characteristic for α,β -unsaturated cyclic ketones bearing alkyl substituents on the C-atoms involved. Apart from this, the spectral data of **25** were almost congruent with those reported for **21**. In addition, a characteristic $[\alpha]_{\text{D}}$ value of -106.2 indicated a close structural relationship to **21** (-110.9). Compound **25** was, thus, determined to be 3-ethyl-1,4-dimethylbicyclo[3.2.1]oct-3-en-2-one, identical with the hypothetical side product **23** in the pyrolysis of **4**. In sharp contrast to the thermal conversion of the vinyl substrates **1**, **16**, **3**, and **4**, the spectral data provided *no* evidence for a propargylic alcohol function formed by homolytic cleavage of $\text{C}(2)–\text{C}(3)$ in **6**.

As illustrated in *Fig. 6*, the exact three-dimensional structural features of both compounds **24** and **25** were established by ^1H -NOE measurements. Irradiation of $\text{C}(1')–\text{Me}$ at $\delta(\text{H})$ 1.26 in **24** produced an NOE effect for the methine H-atom at $\text{C}(3')$, indicating a *cis*-relationship between the propenone and the isopropenyl groups. Compound **25** showed an NOE effect between the vinylic Me group and $\text{H}–\text{C}(5)$ at $\delta(\text{H})$ 2.66, indicating that the Me group was at $\text{C}(4)$, whereas the Et group was ascertained to be at the α -position of the enone moiety.

To better understand the exact course of the above unusual multi-step thermal transformation leading to **25**, we performed both ^2H - and ^{13}C -labeling experiments (*Schemes 21* and *22*). Since the formation of **24** involves only a well-known *retro-ene* step, we will concentrate in the following on the formation of the intriguing bicyclic enone **25**.

Fig. 6. Diagnostic ^1H -NOE correlations of **24** and **25**

The *O*-deuterated ethynylfenchol derivative [*O*- ^2H]-**6** was prepared by repeated treatment of the unlabeled compound with MeOD and D_2O ²⁵). The labeled substrate [$2'$ - ^2H]-**6**, bearing a ^2H -atom in the terminal alkyne position, was obtained by adding a 1:1 mixture of D_2O and MeOD to the freshly prepared lithium acetylide of **6** at -60° (Scheme 21)²⁶). Thermal isomerization of [*O*- ^2H]-**6** gave deuterated **25**, which exhibited two broad *singlets* in the ^2H -NMR spectrum at $\delta(\text{D})$ 1.96 and 0.87 in a relative ratio of *ca.* 1:1. This indicated a 1:1 mixture of [$2'$ - ^2H]- and [$3'$ - ^2H]-**25**. In contrast, pyrolysis of [$2'$ - ^2H]-**6** afforded a single product, [$1'$ - ^2H]-**25**, which showed a *singlet* at $\delta(\text{D})$ 2.19 in its ^2H -NMR spectrum.



^{13}C -Labeled **6** was prepared from (–)-fenchone by addition of Me_3Si -protected [$^{13}\text{C}_2$]-acetylene²⁷) according to the procedure for the unlabeled analogue (Scheme 22). Cleavage of the Me_3Si group was accomplished with TBAF in THF at -10° , affording [$^{13}\text{C}_2$]-**6** in *ca.* 95% yield over two steps²⁸). When the $^{13}\text{C}_2$ -labeled substrate was subjected to DGPTI at 620° , the labels were found to be fully incorporated at C(3) and

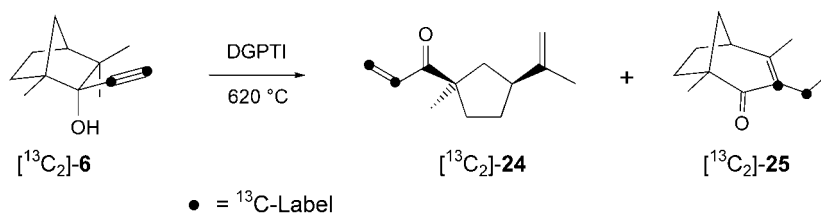
²⁵) The deuterium content was determined by GC/MS to be $>80\%$.

²⁶) The deuterium content was determined by ^1H -NMR to be $>99\%$.

²⁷) Purchased from Cambridge Isotopes (^{13}C -content $>99\%$).

²⁸) The ^{13}C -NMR spectrum revealed two *doublets* at $\delta(\text{C})$ 85.6 and 74.9, with a $^1J(\text{C},\text{C})$ value of 167.4 Hz (*cf. Exper. Part*).

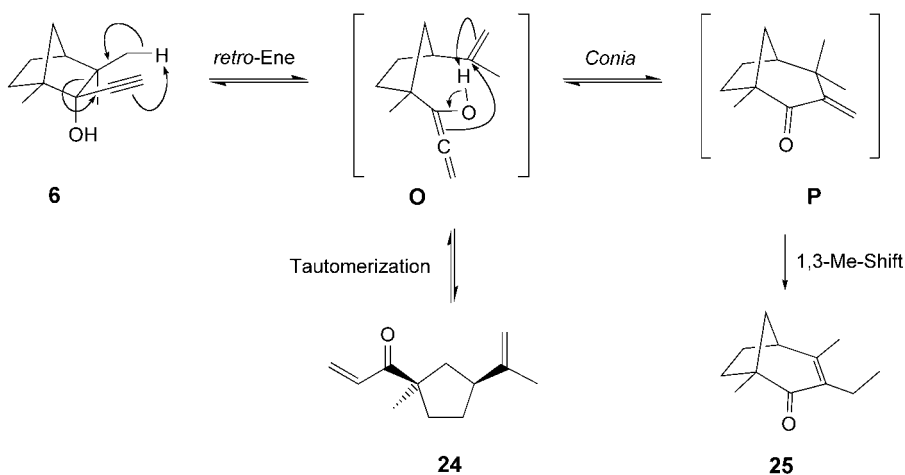
Scheme 22



C(1'). The ^{13}C -NMR spectrum showed a pair of *doublets* at $\delta(\text{C})$ 133.6 and 18.0, respectively, with a $^1J(\text{C,C})$ value of 45.5 Hz. A coupling of 68.2 Hz was observed in the ^{13}C -NMR spectrum of the *retro-ene* product [$^{13}\text{C}_2$]-**24**.

The above results with the labeled compounds are consistent with a mechanism including an initial *retro-ene* reaction under cleavage of the C(2)–C(3) bond of **6** (Scheme 23). In contrast to the *retro-ene* reaction displayed in Scheme 3, the $\text{C}\equiv\text{C}$ bond involved in this process probably gives rise to the intermediate **O** with a hydroxyallene substructure, which is responsible for the formation of the corresponding vinyl ketone **24** by tautomerization in the condensed phase.

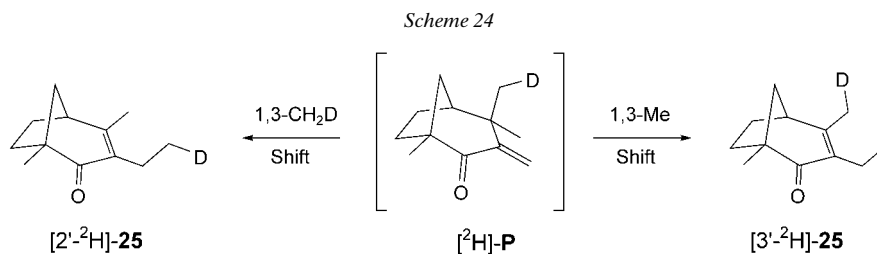
Scheme 23



A competing reaction pathway is assumed to involve a subsequent *Conia* reaction, leading to the *exo*-methyldene intermediate **P**. Driven by the large increase in thermodynamic stability by passing from the hypothetical **P** to the by far more-relaxed **25** ($\Delta\Delta G_{893} = 11.7 \text{ kcal mol}^{-1}$), a 1,3-Me shift might occur under the conditions applied²⁹. If we assume that the *Conia* reaction proceeds stereoselectively, as

²⁹) Only very few examples of 1,3-C shift reactions are reported in the literature. As it is well known, 1,3-migration in sigmatropic rearrangements is necessarily suprafacial due to geometric reasons. In agreement with the *Woodward–Hoffmann* rules, this process has to occur under inversion of configuration of the migrating center [40–43].

corroborated in the case of [O - ^2H]-**1** (Scheme 5), pyrolysis of [O - ^2H]-**6** would, thus, lead to intermediate [^2H]-**P**, carrying the label exclusively in its *exo*-Me group at C(4). However, the observation that the thermal isomerization of [O - ^2H]-**6** gave a 1:1 mixture of [$2'$ - ^2H]- and [$3'$ - ^2H]-**25** provided evidence that the proposed 1,3-Me shift involved the migration of both the *exo*- and the *endo*-Me groups at C(3) of deuterated **P**, as illustrated in Scheme 24.



Although the proposed intermediate **P** could not be detected spectroscopically, its transitory nature on the way to the isolated product **25** seems to be plausible. A qualitative energy profile of the presumed three-step reaction mechanism from **6** to **25** is displayed in Fig. 7.

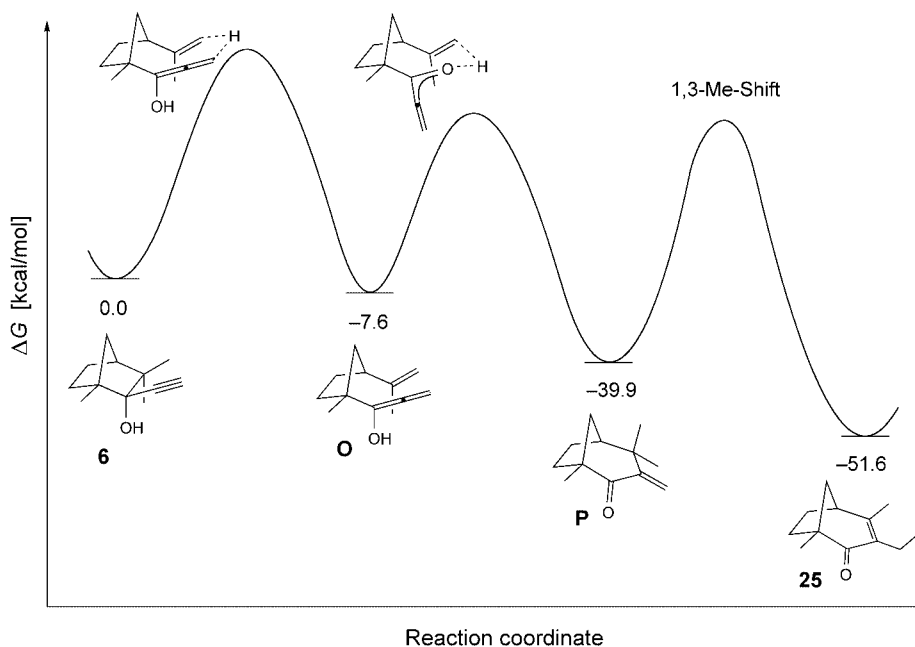
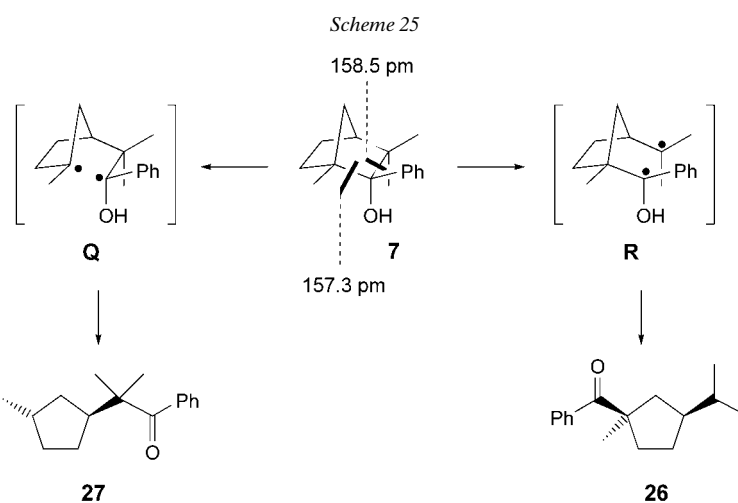


Fig. 7. Energy profile for the conversion of **6** to **25** via different transition states

It is further noteworthy to state that [(trimethylsilyl)ethynyl]fenchol **5** decomposed under DGPTI conditions. Not even traces of the expected mono- and bicyclic products could be observed. Lower reactor temperatures gave rise to unreacted starting

material³⁰⁾ accompanied by a large number of low-boiling side products, while higher temperatures provided an increasing number of unidentified side products.

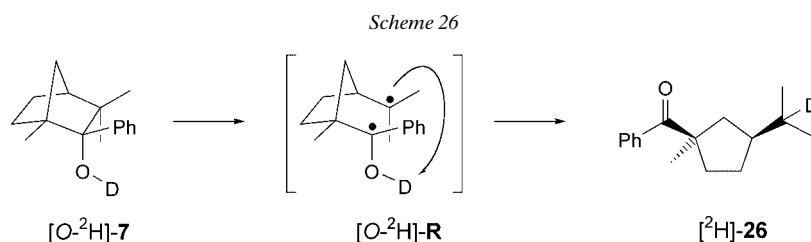
2.2.3. *Isomerization of 2-Phenylfenchol (7)*. As we have very recently reported, the aromatic nature of the phenyl system does not allow concerted pericyclic processes such as *retro-ene* or *Conia* reactions. DGPTI of 2-phenylisoborneol was found to effect clean homolysis of the higher-substituted C(1)–C(2) bond under formation of a diradical intermediate, which underwent intramolecular H-transfer to form a monocyclic acetophenone derivative [23]. Since the α - and α' -positions adjacent to the C=O group in fenchone are both quaternary, a more-competitive partitioning of the cleavage aptitudes was anticipated from the outset. As the homolytic cleavage of both the C(1)–C(2) and the C(2)–C(3) bond in **7** would lead to a diradical intermediate consisting of a hydroxybenzyl and a tertiary-alkyl radical, the formation of two isomeric products had to be expected upon thermo-isomerization of **7** (Scheme 25). Contrarily, AM1 calculations showed that the C(1)–C(2) bond of **7** is shorter (157.3 pm) than the C(2)–C(3) bond (158.5 pm), consistent with reported X-ray crystallographic analyses of phenylfenchol derivatives [44]. Therefore, the intermediate **R** might be favored over **Q**.



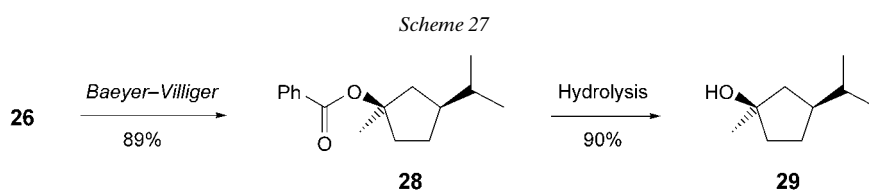
Indeed, when **7** was subjected to DGPTI at 630°, only a single isomerization product (47%) was obtained, accompanied by a variety of low-molecular-weight products. Compound **26** was readily removed from the unpolar side products by chromatography. Its ¹H-NMR spectrum displayed a pair of *doublets* at $\delta(\text{H})$ 0.90 and 0.89, respectively, indicating an *i*-Pr residue with diastereotopic Me groups; and a *singlet* at $\delta(\text{H})$ 1.42 provided evidence for an isolated Me group. The ¹³C-NMR (DEPT) spectrum contained a downfield-shifted *singlet* at $\delta(\text{C})$ 54.7. These data are compatible with methanone **26** rather than ethanone **27**. The formation of the latter was not observed even at more-elevated temperatures.

³⁰⁾ Approximately 10% at 550°, and 30% at 500°, respectively.

The above reaction mechanism was further supported by a deuterium-labeling experiment. As shown in *Scheme 26*, DGPTI of [*O*-²H]-**7** afforded [²H]-**26**. The ²H-NMR spectrum showed that the label was entirely introduced into the *i*-Pr group, appearing as a broad *singlet* at $\delta(D)$ 1.38. Hence, we can state that the weakest single bond in **7** is the C(2)–C(3) bond.

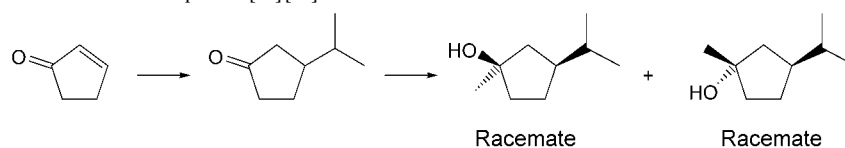


Since phenone **26** represents a versatile chiral building block for the construction of new optically active target molecules, we investigated its derivatization to a more generally applicable form. As we have recently reported [23], the *Baeyer–Villiger* oxidation is a convenient tool to appropriately functionalize such substrates (*Scheme 27*). Treatment of **26** with 3-chlorobenzenecarboperoxoic acid (MCPBA) and 1 equiv. of CF₃COOH (TFA) in CH₂Cl₂ at room temperature afforded benzoate **28** in 89% yield [45]. It is noteworthy to state that the *Baeyer–Villiger* oxidation proceeded regioselectively, *i.e.*, no migration of the Ph group to form the isomeric phenyl ester occurred under these conditions. Subsequent hydrolysis of **28** with LiOH in a 1:1 mixture of MeOH/H₂O at 0° finally afforded the enantiomerically pure *cis*-cyclopentanol **29** in 90% yield [46]³¹).



3. Conclusions. – We have discovered a novel, thermally promoted domino *retro*-ene–*Conia* rearrangement that can be implemented to produce optically active bicyclo[3.2.1]octan-2-ones from easily available bicyclo[2.2.1]heptan-2-ols. The key

³¹) The standard procedure for the preparation of racemic **29** involves 1,4-addition of isopropyl cuprate to cyclopentenone, followed by 1,2-addition of MeMgI to the intermediate 3-isopropylcyclopentanone. Although exclusive *anti*-attack of the nucleophile would be expected to occur, the formation of both diastereoisomers was reported [47][48].



step of this multi-stage protocol consists of a *Conia* rearrangement, involving a one-carbon ring expansion within monocyclic enol-ene intermediates. In cases where the ring-expanded products are sterically too congested, unusual subsequent reactions, e.g., dealkylations or 1,3-C shifts, allow the system to relax. The observation that this fragmentation/recyclization process occurs, despite temperatures above 600°, with no loss of optical activity makes the presented domino *retro-ene*–*Conia* rearrangement an interesting method for the construction of a broad variety of chiral building blocks. Further studies of DGPTI processes involving other substrates are in progress.

We thank our NMR laboratory, in particular *N. Walch*, Dr. *G. Hopp-Rentsch*, and *S. Jurt*, for specific measurements, as well as the MS department and the laboratory of microanalysis. Financial support by the *Swiss National Science Foundation* is gratefully acknowledged.

Experimental Part

1. *General*. See [49].

2. *Monoterpene Substrates*. 2.1. *General Procedure (GP 1) for the Addition of 1-Alkenyl Grignard Reagents to (–)-Fenchone*. A 1.0M soln. of the *Grignard* reagent was prepared by treating a suspension of Mg (1.20 g, 49.3 mmol) in anh. THF (49 ml) with the corresponding 1-alkenyl bromide (49.3 mmol) at r.t. In a separate flask, (–)-fenchone (5.0 g, 32.8 mmol) was added with stirring to a suspension of CeCl₃ (6.5 g, 26.3 mmol) in THF (100 ml) at r.t. Stirring was continued for 0.5–2 h, after which the initially yellowish suspension became homogenous and yogurt-like. To this mixture, the freshly prepared 1-alkenyl magnesium bromide soln. was added *via* cannula at r.t., while the temperature rose to 45°. Stirring was continued for 1 h. The resulting ivory-colored suspension was then poured into a separatory funnel containing crushed ice, H₂O (500 ml), and Et₂O (200 ml). A 10% aq. HCl soln. was added with stirring until the mixture became clear (pH < 3). The org. layer was washed with H₂O (2 ×). The aq. layers were extracted with Et₂O (3 × 50 ml). The combined org. layers were washed with a sat. soln. of NaHCO₃ and brine, dried (MgSO₄), filtered, and evaporated under reduced pressure.

2.2. *(1R,2R,4S)-2-Ethenyl-1,3,3-trimethylbicyclo[2.2.1]heptan-2-ol (1)*. *GP 1*, with 4.70 g (30.9 mmol) of (–)-fenchone and a commercially available 1M soln. of vinyl magnesium bromide in THF. The crude product was filtered through a pad of SiO₂ using hexane/AcOEt 40:1 to give **1** (5.29 g, 95%) as a colorless oil. [α]_D²³ = –12.0 (*c* = 1.0, CH₂Cl₂). IR (film): 3505s, 3085m, 2959vs, 2874vs, 1633m, 1472vs, 1460vs, 1410s, 1384vs, 1319s, 1261s, 1169s, 1134vs, 1100vs, 1080vs, 1022s, 994vs, 912vs, 836s, 812m. ¹H-NMR (600 MHz, CDCl₃): 5.99 (*dd*, ³*J*_{trans} = 17.2, ³*J*_{cis} = 10.9, H–C(1′)); 5.57 (*dd*, ³*J*_{trans} = 17.2, ²*J* = 1.6, H_{trans}–C(2′)); 5.04 (*dd*, ³*J*_{cis} = 10.9, ²*J* = 1.6, H_{cis}–C(2′)); 1.98 (*dddd*, *J* = 12.6, 11.8, 5.5, 2.9, H_{endo}–C(5)); 1.78–1.72 (*m*, H–C(4), H_{endo}–C(6), H_{syn}–C(7)); 1.48–1.42 (*m*, H_{exo}–C(6)); 1.24 (*s*, OH); 1.18 (*dd*, *J* = 11.5, 1.6, H_{anti}–C(7)); 1.07 (*td*, *J* = 12.6, 3.6, H_{exo}–C(5)); 0.92 (*s*, Me–C(1)); 0.89 (*s*, Me_{exo}–C(3)); 0.88 (*s*, Me_{endo}–C(3)). ¹³C-NMR (150 MHz, CDCl₃): 142.9 (*d*, C(1′)); 110.1 (*t*, C(2′)); 82.5 (*s*, C(2)); 52.2 (*s*, C(3)); 48.4 (*d*, C(4)); 44.4 (*s*, C(1)); 40.6 (*t*, C(7)); 29.2 (*t*, C(5)); 28.6 (*q*, Me_{endo}–C(3)); 25.5 (*t*, C(6)); 21.9 (*q*, Me–C(1)); 17.2 (*q*, Me_{exo}–C(3)). EI-MS: 180 (2, *M*⁺), 165 (11, [*M*–CH₃]⁺), 137 (14), 123 (9), 109 (15), 97 (100), 81 (98), 69 (41), 55 (87). Anal. calc. for C₁₂H₂₀O (180.29): C 79.94, H 11.18; found: C 79.81, H 11.08.

2.3. *(1R,2R,4S)-1,3,3-Trimethyl-2-[(E)-prop-1-en-1-yl]bicyclo[2.2.1]heptan-2-ol ((E)-2) and (1R,2R,4S)-1,3,3-Trimethyl-2-[(Z)-prop-1-en-1-yl]bicyclo[2.2.1]heptan-2-ol ((Z)-2)*. *GP 1*, with 4.70 g (30.5 mmol) of (–)-fenchone. The crude product was filtered through a pad of SiO₂ using hexane/AcOEt 40:1 to give **2** (5.45 g, 92%) as a 1:1 mixture of (*E*)- and (*Z*)-isomers. An anal. sample of each component was obtained by CC (SiO₂; hexane/AcOEt 60:1).

Data of (Z)-2. [α]_D²³ = –28.6 (*c* = 1.0, CH₂Cl₂). IR (film): 3513w, 3023m, 2961vs, 2873vs, 1648w, 1460vs, 1385s, 1319m, 1274s, 1199w, 1123s, 1101s, 1050s, 1028s, 1010s, 996vs, 914s, 837m, 750m. ¹H-NMR (600 MHz, CDCl₃): 5.52 (*dq*, ³*J*_{cis} = 11.9, ³*J* = 7.0, H–C(2′)); 5.43 (*dq*, ³*J*_{cis} = 11.9, ⁴*J* = 1.6, H–C(1′)); 1.98 (*dddd*, *J* = 15.0, 12.7, 5.8, 2.3, H_{endo}–C(5)); 1.85 (*dd*, ³*J* = 7.0, ⁴*J* = 1.6, Me(3′)); 1.75–1.69 (*m*, H_{endo}–C(6)); 1.65–1.61 (*m*, H–C(4), H_{syn}–C(7)); 1.40 (*dddd*, *J* = 12.7, 11.2, 5.7, 3.9, H_{exo}–C(6)); 1.30 (*br. s*, OH); 1.12 (*dd*, *J* = 10.2, 1.2, H_{anti}–C(7)); 1.08 (*td*, *J* = 12.7, 3.9, H_{exo}–C(5)); 1.02 (*s*, Me–C(1)); 0.98 (*s*, Me_{exo}–C(3)); 0.88 (*s*, Me_{endo}–C(3)). ¹³C-NMR (150 MHz, CDCl₃): 134.5 (*d*, C(1′)); 125.2 (*d*, C(2′)); 83.9 (*s*, C(2)); 53.2 (*s*, C(3)); 48.7 (*d*, C(4)); 44.5 (*s*, C(1)); 40.5 (*t*, C(7)); 29.5 (*q*, Me_{endo}–C(3)); 28.9 (*t*, C(5)); 25.7 (*t*, C(6));

22.8 (*q*, *Me*-C(1)); 16.8 (*q*, *Me*_{exo}-C(3)); 15.2 (*q*, C(3')). EI-MS: 194 (3, *M*⁺), 179 (6, [*M*-CH₃]⁺), 151 (10), 123 (23), 111 (97), 97 (24), 81 (78), 69 (100), 55 (37).

Data of (*E*)-**2**. [α]_D²³ = -31.0 (*c* = 1.0, CH₂Cl₂). IR (film): 3513w, 3030m, 2961vs, 2872vs, 1460s, 1377m, 1328m, 1264m, 1199w, 1166w, 1131m, 1100m, 1066m, 1025m, 1007s, 981s, 924m, 739w. ¹H-NMR (600 MHz, CDCl₃): 5.60–5.56 (*m*, H-C(1'), H-C(2')); 1.96 (*dddd*, *J* = 12.5, 11.0, 5.5, 2.4, H_{endo}-C(5)); 1.76–1.65 (*m*, Me(3'), H-C(4), H_{endo}-C(6), H_{syn}-C(7)); 1.43 (*dddd*, *J* = 16.5, 12.4, 5.3, 4.3, H_{exo}-C(6)); 1.21 (*br. s*, OH); 1.15 (*dd*, *J* = 10.2, 1.4, H_{anti}-C(7)); 1.05 (*td*, *J* = 12.5, 3.6, H_{exo}-C(5)); 0.90 (*s*, Me-C(1)); 0.87 (*s*, Me₂C(3)). ¹³C-NMR (150 MHz, CDCl₃): 136.1 (*d*, C(1')); 120.5 (*d*, C(2')); 81.8 (*s*, C(2)); 52.4 (*s*, C(3)); 48.6 (*d*, C(4)); 44.7 (*s*, C(1)); 40.7 (*t*, C(7)); 29.3 (*t*, C(5)); 28.9 (*q*, Me_{endo}-C(3)); 25.7 (*t*, C(6)); 22.1 (*q*, Me-C(1)); 17.7 (*q*, C(3')); 17.4 (*q*, Me_{exo}-C(3)). EI-MS: 194 (2, *M*⁺), 179 (5, [*M*-CH₃]⁺), 151 (8), 123 (14), 111 (91), 97 (19), 81 (65), 69 (100), 55 (40).

2.4. (*IR*,*2R*,*4S*)-*1,3,3*-Trimethyl-2-(1-methylethenyl)bicyclo[2.2.1]heptan-2-ol (**3**). *GP I*, with 5.00 g (32.8 mmol) of (-)-fenchone. The crude product was filtered through a pad of SiO₂ using hexane/AcOEt 40:1 to give **3** (6.13 g, 96%) as a colorless oil. [α]_D²³ = -18.9 (*c* = 1.0, CH₂Cl₂). IR (film): 3506m, 3105w, 2962vs, 2932vs, 2876vs, 1637m, 1464vs, 1386s, 1366s, 1316m, 1295m, 1240w, 1197w, 1159w, 1110w, 1063s, 1031m, 1009s, 978s, 952m, 903vs, 831w. ¹H-NMR (600 MHz, CDCl₃): 5.01 (*t*, *J* = 1.5, H-C(2'), NOE with Me-C(1')); 4.97 (*s*, H-C(2')); 2.13–2.04 (*m*, H_{endo}-C(5)); 2.03 (*dq*, *J* = 10.4, 2.0, H_{syn}-C(7)); 1.81 (*s*, Me-C(1')); 1.70–1.63 (*m*, H-C(4), H_{endo}-C(6)); 1.41–1.38 (*m*, H_{exo}-C(6)); 1.32 (*td*, *J* = 12.6, 3.6, H_{exo}-C(5)); 1.18 (*dd*, *J* = 10.4, 1.4, H_{anti}-C(7)); 0.99 (*s*, Me_{exo}-C(3)); 0.98 (*s*, Me-C(1)); 0.93 (*s*, Me_{endo}-C(3)). ¹³C-NMR (150 MHz, CDCl₃): 144.9 (*s*, C(1')); 112.3 (*t*, C(2')); 85.1 (*s*, C(2)); 52.4 (*s*, C(3)); 49.6 (*d*, C(4)); 44.6 (*s*, C(1)); 41.3 (*t*, C(7)); 30.2 (*t*, C(5)); 28.9 (*q*, Me_{endo}-C(3)); 26.9 (*t*, C(6)); 24.9 (*q*, Me-C(1)); 23.8 (*q*, Me-C(1')); 22.2 (*q*, Me_{exo}-C(3)). EI-MS: 194 (5, *M*⁺), 179 (12, [*M*-CH₃]⁺), 151 (16), 123 (59), 111 (92), 95 (30), 81 (100), 69 (96), 55 (61). Anal. calc. for C₁₃H₂₂O (194.32): C 80.35, H 11.41; found: C 80.22, H 11.36.

2.5. (*IR*,*2R*,*4S*)-*1,3,3*-Trimethyl-2-[(*E*)-1-methylprop-1-en-1-yl]bicyclo[2.2.1]heptan-2-ol (**4**). A flame-dried flask was flushed with Ar gas and charged with Li dispersion (30% in mineral oil, 0.33 g, 47.1 mmol). After washing the Li dispersion with anhyd. Et₂O (3 × 20 ml), Et₂O (30 ml) was transferred into the flask, and (*E/Z*)-2-bromobut-2-ene (2.44 ml, 21.4 mmol) was added dropwise under vigorous stirring at r.t. The resulting grey suspension was stirred for 2 h at r.t. The precipitated LiBr was allowed to settle, and the resulting soln. was transferred by cannula through a glass-wool pad into a flask cooled to -20°, containing a suspension of (-)-fenchone (2.5 g, 11.9 mmol) and CeCl₃ (3.23 g, 13.1 mmol) in THF (25 ml). This mixture was then warmed to r.t. and stirring was continued for 5 h at that temp. The resulting dark-red suspension was poured into a separatory funnel containing crushed ice, H₂O (200 ml), and Et₂O (100 ml). A 10% aq. HCl soln. was added with stirring until the mixture became clear (pH < 3). The org. layer was washed with H₂O (2 ×). The aq. layers were extracted with Et₂O (2 × 50 ml). The combined org. layers were washed with a sat. soln. of NaHCO₃ and brine, dried (MgSO₄), filtered, and evaporated under reduced pressure. The residue was purified by CC (hexane/AcOEt 40:1) to give (*E*)-**4** (1.07 g, 43%) as a colorless oil. A minor amount (ca. 15%) of (*Z*)-**4** was evident from ¹H- and ¹³C-NMR analyses. [α]_D²³ = -23.6 (*c* = 1.0, CH₂Cl₂). IR (film): 3562s, 3026s, 2952vs, 2873vs, 1464vs, 1385s, 1375s, 1364s, 1347m, 1320m, 1262m, 1233m, 1205m, 1163w, 1114m, 1057vs, 1030s, 1007vs, 970vs, 903w, 876w, 811w. ¹H-NMR (600 MHz, CDCl₃): 5.59–5.57 (*m*, H-C(2')); 2.05 (*dddd*, *J* = 12.6, 11.4, 5.8, 2.3, H_{endo}-C(5)); 1.79–1.68 (*m*, H_{endo}-C(6), Me-C(1',2')); 1.62–1.56 (*m*, H-C(4), H_{syn}-C(7)); 1.46–1.37 (*m*, H_{exo}-C(6)); 1.09 (*dd*, *J* = 11.1, 1.2, H_{anti}-C(7)); 1.07 (*s*, Me_{endo}-C(3)); 1.02–0.95 (*m*, H_{exo}-C(5)); 1.01 (*s*, Me_{exo}-C(3)); 0.91 (*s*, Me-C(1)). ¹³C-NMR (150 MHz, CDCl₃): 145.0 (*s*, C(1')); 130.3 (*d*, C(2')); 79.5 (*s*, C(2)); 52.4 (*s*, C(3)); 50.3 (*d*, C(4)); 44.6 (*s*, C(1)); 41.3 (*t*, C(7)); 30.9 (*t*, C(5)); 28.0 (*q*, Me_{endo}-C(3)); 25.3 (*t*, C(6)); 23.02, 22.97 (2*q*, Me-C(1), Me_{exo}-C(3)); 18.44, 18.38 (2*q*, Me-C(1',2')). EI-MS: 208 (7, *M*⁺), 194 (2), 165 (4), 153 (48), 135 (6), 125 (43), 109 (15), 95 (13), 81 (71), 69 (100), 55 (50).

2.6. (*IR*,*2R*,*4S*)-*1,3,3*-Trimethyl-2-[(trimethylsilyl)ethynyl]bicyclo[2.2.1]heptan-2-ol (**5**). To a stirred soln. of 1-(trimethylsilyl)ethyne (5.28 ml, 38.18 mmol) in anhyd. THF (200 ml), a 2.4M soln. of BuLi in hexane (15.11 ml, 36.28 mmol) was slowly added *via* syringe at -10°. The resulting pale yellow lithium acetylide soln. was stirred for 30 min at -10°, and then added *via* cannula to a suspension of (-)-fenchone (4.36 g, 28.63 mmol) and CeCl₃ (5.65 g, 22.92 mmol) in THF (140 ml), as described in *GP I*. The crude product was filtered through a pad of silica gel using hexane/AcOEt 40:1 to give **5** (7.10 g, 99%) as a dark-yellow oil. [α]_D²³ = +17.2 (*c* = 1.0, CH₂Cl₂). IR (film): 3476m, 2960vs, 2932vs, 2900s, 2874s, 2164m, 1461s, 1386m, 1376m, 1366m, 1319m, 1304m, 1210w, 1112s, 1064s, 1038s, 1009s, 913w, 858vs, 842vs, 760s, 698w. ¹H-NMR (300 MHz, CDCl₃): 1.94 (*dddd*, *J* = 12.7, 11.3, 5.9, 2.2, H_{endo}-C(5)); 1.82–1.76 (*m*, H-C(4), H_{endo}-C(6), H_{syn}-C(7), OH); 1.39 (*dddd*, *J* = 16.7, 12.6, 6.0, 4.0, H_{exo}-C(6)); 1.28 (*s*, Me-C(1)); 1.23 (*s*, Me_{exo}-C(3)); 1.21 (*dd*, *J* = 10.3, 1.7, H_{anti}-C(7)); 1.20 (*td*, *J* = 12.7, 3.7, H_{exo}-C(5)); 1.05 (*s*, Me_{endo}-C(3)); 0.26 (*s*, Me₃Si). ¹³C-NMR (75 MHz, CDCl₃): 107.8

(s, C(2')); 91.1 (s, C(1')); 80.9 (s, C(2)); 53.3 (s, C(3)); 48.6 (d, C(4)); 43.1 (s, C(1)); 41.2 (t, C(7)); 30.0 (q, Me_{exo} -C(3)); 27.2 (t, C(5)); 25.9 (t, C(6)); 21.7 (q, Me_{endo} -C(3)); 18.0 (q, Me -C(1)); 0.0 (q, Me_3Si). EI-MS: 250 (1, M^{+}), 235 (58, $[M - CH_3]^{+}$), 219 (10), 207 (13), 167 (82), 123 (11), 99 (52), 81 (68), 73 (100).

2.7. (1*R*,2*R*,4*S*)-1,3,3-Trimethyl-2-[(trimethylsilyl)]¹³C₂ethynylbicyclo[2.2.1]heptan-2-ol (¹³C₂]-5). This compound was prepared in analogy to unlabeled **5**, from 1-(trimethylsilyl)]¹³C₂ethyne. ¹³C-NMR (75 MHz, CDCl₃): 107.8 (d, ²J(C,C) = 129.1, C(2')); 91.1 (d, ²J(C,C) = 129.1, C(1')). EI-MS: 252 (1, M^{+}), 237 (30, $[M - CH_3]^{+}$), 221 (5), 209 (10), 193 (4), 169 (67), 155 (15), 141 (9), 123 (11), 101 (47), 82 (88), 75 (93), 73 (100), 69 (20), 55 (16).

2.8. (1*R*,2*R*,4*S*)-2-Ethynyl-1,3,3-trimethylbicyclo[2.2.1]heptan-2-ol (**6**). To a stirred soln. of **5** (6.49 g, 25.9 mmol) in THF (250 ml) was added tetrabutylammonium fluoride trihydrate (TBAF; 8.18 g, 25.9 mmol) at -10°. The colorless soln. was allowed to warm to r.t. and was then stirred at this temp. for 30 min. The mixture was poured into a separatory funnel containing crushed ice and Et₂O (100 ml). The org. layer was separated, and the aq. phase was extracted with Et₂O (3 × 100 ml). The combined org. layers were washed with H₂O and brine, dried (MgSO₄), filtered, and concentrated *in vacuo*. The crude product was filtered through a pad of SiO₂ using hexane/AcOEt 80 : 1 to give **6** (4.53 g, 98%) as a slightly yellow oil. [α]_D²⁵ = +19.6 (c = 1.0, CH₂Cl₂). IR (film): 3457s, 3308vs, 2961vs, 2932vs, 2874vs, 2104vw, 1460s, 1387m, 1377m, 1366m, 1330m, 1252m, 1111m, 1062vs, 1030s, 1010vs, 1000s, 914m, 884m, 841w, 649m. ¹H-NMR (600 MHz, CDCl₃): 2.55 (s, H-C(2')); 1.91 (dddd, J = 12.7, 11.3, 6.0, 2.2, H_{endo}-C(5)); 1.83 (br. s, OH); 1.74 (dq, J = 10.2, 1.9, H_{syn}-C(7)); 1.72–1.68 (m, H-C(4)); 1.67 (tt, J = 16.0, 2.9, H_{endo}-C(6)); 1.40 (dddd, J = 16.0, 12.5, 6.0, 4.1, H_{exo}-C(6)); 1.20 (s, Me-C(1)); 1.15 (s, Me_{exo}-C(3)); 1.14 (dd, J = 10.2, 1.6, H_{anti}-C(7)); 1.12 (td, J = 12.7, 3.7, H_{exo}-C(5)); 0.96 (s, Me_{endo}-C(3)). ¹³C-NMR (150 MHz, CDCl₃): 85.6 (s, C(1')); 80.6 (s, C(2)); 74.9 (d, C(2')); 53.2 (s, C(3)); 48.5 (d, C(4)); 43.0 (s, C(1)); 41.0 (t, C(7)); 29.9 (q, Me_{exo}-C(3)); 27.2 (t, C(5)); 25.8 (t, C(6)); 21.5 (q, Me_{endo}-C(3)); 17.9 (q, Me-C(1)). EI-MS: 178 (1, M^{+}), 163 (11, $[M - CH_3]^{+}$), 135 (29), 121 (5), 107 (22), 96 (75), 81 (100), 67 (32), 53 (50).

2.9. (1*R*,2*R*,4*S*)-2-([2-²H]Ethynyl)-1,3,3-trimethylbicyclo[2.2.1]heptan-2-ol ([2-²H]-6). A soln. of **6** (0.713 g, 3.0 mmol) in anh. THF (10 ml) was cooled to -78°. A 2.4M soln. of BuLi in hexane (5.0 ml, 12 mmol) was slowly added *via* syringe. The yellow soln. was stirred for 1 h at -40°, and cooled to -78°. A 1 : 1 mixture of D₂O/MeOD (1 ml) was added dropwise. The mixture was then allowed to warm to r.t. within 2 h. Workup in the usual fashion afforded [2-²H]-6 (0.712 g, quant.) as a yellow oil. IR (film): 3474m, 3308w, 2960vs, 2932vs, 2873vs, 2591s, 1965vw, 1459s, 1386m, 1377m, 1366m, 1319m, 1261m, 1111m, 1061vs, 1030s, 1009vs, 999s, 914m, 884m, 825w, 649vw. ²H-NMR (600 MHz, CDCl₃): 2.55 (s, D-C(2')). EI-MS: 179 (1, M^{+}), 164 (17, $[M - CH_3]^{+}$), 151 (8), 136 (39), 122 (11), 108 (28), 96 (75), 95 (76), 81 (100), 69 (25), 54 (31).

2.10. (1*R*,2*R*,4*S*)-2-([¹³C₂]Ethynyl)-1,3,3-trimethylbicyclo[2.2.1]heptan-2-ol ([¹³C₂]-6). Prepared in analogy to unlabeled **6**. ¹³C-NMR (75 MHz, CDCl₃): 85.6 (d, ²J(C,C) = 167.4, C(1')); 74.9 (d, ²J(C,C) = 167.4, C(2')). EI-MS: 179 (1, M^{+}), 165 (14, $[M - CH_3]^{+}$), 152 (12), 137 (51), 123 (13), 109 (29), 98 (87), 97 (80), 83 (72), 81 (100), 69 (46), 67 (31), 55 (78), 53 (24).

2.11. (1*R*,2*R*,4*S*)-1,3,3-Trimethyl-2-phenylbicyclo[2.2.1]heptan-2-ol (**7**). A soln. of PhLi was prepared by the dropwise addition of bromobenzene (3.14 g, 20 mmol) to a Li dispersion (50 mmol) in Et₂O (20 ml) at r.t., followed by stirring at r.t. for 1 h. The generated LiBr and excess Li were filtered off under Ar. The resulting soln. was diluted with toluene (20 ml) and hexane (10 ml), and cooled to 10°. (-)-Fenchone (2.5 g, 16.42 mmol) dissolved in toluene (20 ml) was added slowly to keep the temp. below 20°. The mixture was allowed to warm to r.t. within 1 h, and stirring was continued for 2 h. The reaction was quenched with sat. aq. NH₄Cl soln., and the mixture was diluted with Et₂O. The separated org. phase was washed with brine, dried (MgSO₄), and evaporated. CC (SiO₂; hexane/AcOEt 30 : 1) afforded **7** (3.37 g, 89%) as a colorless oil. [α]_D²⁵ = -38.0 (c = 2.0, hexane). IR (film): 3599s, 3555s, 3495s, 3058s, 2962vs, 2974vs, 1600m, 1464vs, 1386s, 1312s, 1088m, 1051vs, 1013vs, 907s, 749vs, 707vs. ¹H-NMR (300 MHz, CDCl₃): 7.57 (A of AA'BB'C, 2 H_o of Ph); 7.49 (B of AA'BB'C, 2 H_m of Ph); 7.28 (C of AA'BB'C, H_p of Ph); 2.32 (br. d, J = 10.5, H_{syn}-C(7)); 2.19 (dddd, J = 12.5, 10.9, 5.7, 2.9, H_{endo}-C(5)); 1.83–1.75 (m, H-C(4), H_{endo}-C(6)); 1.61 (s, OH); 1.60–1.40 (m, H_{exo}-C(6)); 1.37 (dd, J = 10.5, 1.5, H_{anti}-C(7)); 1.19 (td, J = 12.5, 4.7, H_{exo}-C(5)); 1.11 (s, Me-C(1)); 1.03 (s, Me₂-C(3)). ¹³C-NMR (75 MHz, CDCl₃): 145.0 (s, C_{ipso} of Ph); 127.5 (d, C_o of Ph); 127.1 (d, C_m of Ph); 125.9 (d, C_p of Ph); 84.0 (s, C(2)); 52.7 (s, C(3)); 48.9 (d, C(4)); 45.6 (s, C(1)); 41.8 (t, C(7)); 33.6 (t, C(5)); 30.0 (q, Me_{endo}-C(3)); 24.0 (t, C(6)); 21.2 (q, Me-C(1)); 17.3 (q, Me_{exo}-C(3)). EI-MS: 230 (8, M^{+}), 212 (20, $[M - H_2O]^{+}$), 169 (21), 147 (84), 123 (63), 105 (100, CPh⁺), 81 (72), 69 (45).

3. Dynamic Gas-Phase Thermo-Isomerizations. 3.1. General Procedure (GP 2) for DGPTI of Fenchol Substrates. The thermo-isomerization device consists of an electrically heatable tube furnace (1-m long), a condenser unit with a cooling trap at the outlet side, and a Kugelrohr oven as the evaporation unit at the inlet

side. A quartz tube (110-cm long, 2.5-cm i.d.), which fitted into the furnace, was connected to a trap (cooled with liquid N₂) on one side and to a bulb placed in the *Kugelrohr* oven on the other. The starting material (typically 2 g) was placed in the bulb equipped with a capillary inlet device for the inert flow gas (N₂) and a magnetic stirrer. After evacuation of the apparatus with a high-vacuum oil pump, the starting material was distilled directly through the preheated reactor tube (1–3 g/h). After all of the starting material had been distilled, the apparatus was vented, and the frozen products were transferred to a bulb with Et₂O as the solvent. The resulting soln. was dried (MgSO₄) and evaporated under reduced pressure. The following parameters are typical for the DGPTI process: *i*) the *Kugelrohr* oven was heated to 100–150°; *ii*) a flow of N₂ was adjusted to 0.8–1.4 l/h; *iii*) the reactor tube was heated to 500–700°; *iv*) the high-vacuum was adjusted to 2–4 × 10⁻² mbar.

3.2. 1-[(1*R*,3*S*)-1-Methyl-3-(1-methylethenyl)cyclopent-1-yl]propan-1-one (**8**), 1-[(1*R*,3*S*)-1-Methyl-3-(1-methylethyl)cyclopent-1-yl]prop-2-en-1-one (**9**), and (1*R*,3*R*,5*S*)-1,3,4,4-Tetramethylbicyclo[3.2.1]octan-2-one (**10**). Following *GP 2*, fenchol **1** (3.00 g, 16.6 mmol) was thermo-isomerized at 620°. The yellow crude product was purified by CC (hexane/AcOEt 40:1) to give **8** (0.30 g), followed by a mixed fraction of **10**/**8** 8:1 (1.21 g), and **9** (0.32 g). A pure sample of **10** was prepared by resubjecting the obtained 8:1-mixture to CC.

Data of 8. $[\alpha]_{\text{D}}^{23} = -8.9$ ($c = 1.0$, CH₂Cl₂). IR (film): 3081vw, 2964vs, 2871s, 1705vs, 1645w, 1458s, 1376m, 1261w, 1080w, 986m, 886m, 737m. ¹H-NMR (600 MHz, CDCl₃): 4.65 (br. s, H of isopropenyl); 4.62 (br. s, H of isopropenyl, NOE with Me of isopropenyl); 2.59–2.55 (*m*, H–C(3')); 2.44 (*q*, ³*J* = 7.3, CH₂(2)); 2.11 (*ddd*, *J* = 12.4, 8.5, 3.3, H_{exo}–C(5')); 1.83–1.79 (*m*, H_{exo}–C(2'), H_{endo}–C(4')); 1.65 (*s*, Me of isopropenyl); 1.56 (*dd*, *J* = 11.9, 6.2, H_{endo}–C(2')); 1.43–1.33 (*m*, H_{exo}–C(4'), H_{endo}–C(5')); 1.18 (*s*, Me–C(1')); 0.99 (*t*, ³*J* = 7.3, Me(3)). ¹³C-NMR (150 MHz, CDCl₃): 214.3 (*s*, C(1)); 146.6 (*s*, C–C(3')); 107.8 (*t*, CH₂ of isopropenyl); 53.9 (*s*, C(1')); 44.9 (*d*, C(3')); 40.2 (*t*, C(2')); 34.8 (*t*, C(5')); 29.9 (*t*, C(4')); 29.5 (*t*, C(2)); 24.6 (*q*, Me–C(1')); 20.0 (*q*, Me of isopropenyl); 8.4 (*q*, C(3)). EI-MS: 180 (2, *M*⁺), 151 (14, [M–C₂H₅]⁺), 123 (51), 107 (15), 95 (7), 81 (100), 67 (37), 57 (40).

Data of 9. $[\alpha]_{\text{D}}^{23} = -6.2$ ($c = 1.0$, CH₂Cl₂). IR (film): 3038w, 2962vs, 2872s, 1690vs, 1645vw, 1612w, 1453s, 1380m, 1275vw, 1015w, 919w, 886m. ¹H-NMR (300 MHz, CDCl₃): 6.63 (*dd*, ³*J*_{trans} = 17.0, ³*J*_{cis} = 10.3, H–C(2)); 6.28 (*dd*, ³*J*_{trans} = 17.0, ²*J* = 2.2, H_{trans}–C(3)); 5.59 (*dd*, ³*J*_{cis} = 10.3, ²*J* = 2.2, H_{cis}–C(3)); 2.12 (*ddd*, *J* = 13.0, 9.0, 3.7, H_{exo}–C(5')); 1.90–1.82 (*m*, H_{endo}–C(4')); 1.72–1.60 (*m*, CH₂(2'), H–C(3)); 1.45–1.37 (*m*, H_{endo}–C(5')); 1.28–1.20 (*m*, H_{exo}–C(4'), Me₂CH); 1.19 (*s*, Me–C(1')); 0.88, 0.87 (*2d*, ³*J* = 6.7, Me₂CH). ¹³C-NMR (75 MHz, CDCl₃): 201.3 (*s*, C(1)); 131.0 (*d*, C(2)); 127.1 (*t*, C(3)); 53.1 (*s*, C(1')); 45.9 (*d*, C(3')); 39.9 (*t*, C(2)); 35.0 (*t*, C(5')); 33.7 (*d*, Me₂CH); 30.6 (*t*, C(4')); 24.1 (*q*, Me–C(1')); 20.54, 20.48 (*2q*, Me₂CH). EI-MS: 180 (2, *M*⁺), 151 (2), 123 (12), 107 (3), 101 (23), 81 (100), 67 (19), 57 (14).

Data of 10. $[\alpha]_{\text{D}}^{23} = -42.8$ ($c = 1.0$, CH₂Cl₂). IR (film): 2965vs, 2873vs, 1698vs, 1461s, 1392m, 1377m, 1369m, 1344w, 1261w, 1198w, 1152w, 1103w, 1012m, 986m, 953w. ¹H-NMR (600 MHz, CDCl₃): 2.25 (*q*, ³*J* = 6.7, H–C(3)); 1.95 (*dddd*, *J* = 16.1, 9.1, 4.8, 2.2, H_{endo}–C(6)); 1.91–1.85 (*m*, H_{exo}–C(6)); 1.83–1.78 (*m*, H–C(5), H_{syn}–C(8)); 1.65 (*dddd*, *J* = 16.3, 9.1, 5.2, 1.9, H_{endo}–C(7)); 1.48 (*ddd*, *J* = 16.3, 12.7, 4.8, H_{exo}–C(7)); 1.46 (*dd*, *J* = 12.4, 4.4, H_{anti}–C(8)); 1.04 (*s*, Me–C(1)); 0.98 (*s*, Me_{endo}–C(4)); 0.84 (*d*, *J* = 6.7, Me–C(3)); 0.69 (*s*, Me_{exo}–C(4)). ¹³C-NMR (150 MHz, CDCl₃): 215.1 (*s*, C(2)); 51.3 (*s*, C(1)); 47.7 (*d*, C(5)); 46.9 (*d*, C(3)); 41.1 (*t*, C(8)); 40.7 (*s*, C(4)); 34.5 (*t*, C(7)); 25.6 (*q*, Me_{endo}–C(4)); 25.4 (*t*, C(6)); 21.3 (*q*, Me_{exo}–C(4)); 18.8 (*q*, Me–C(1)); 7.2 (*q*, Me–C(3)). EI-MS: 180 (2, *M*⁺), 166 (1), 152 (2), 137 (1), 123 (6), 109 (2), 98 (4), 81 (100), 67 (8), 55 (7). HR-EI-MS: 180.1519 (*M*⁺, C₁₂H₂₀O⁺; calc. 180.1514).

3.3. 1-[(1*R*,3*S*)-1-Methyl-3-(1-methylethenyl)cyclopent-1-yl][2-²H]propan-1-one (²H-**8**), 1-[(1*R*,3*S*)-1-Methyl-3-(1-methyl-[1-²H]ethyl)cyclopent-1-yl]prop-2-en-1-one (²H-**9**), and (1*R*,3*R*,4*R*,5*S*)-4-(²H)Methyl-1,3,4-trimethylbicyclo[3.2.1]octan-2-one (²H-**10**). Following *GP 2*, [²H]**1** (1.01 g, 5.57 mmol) was thermo-isomerized at 620°. Purification as described for the unlabeled substrate **1** afforded the pure compounds.

Data of ²H-8. ²H-NMR (600 MHz, CDCl₃): 2.44 (br. s, D–C(2)). EI-MS: 181 (5, *M*⁺), 151 (12, [M–C₂H₄D]⁺), 123 (50), 107 (15), 95 (8), 81 (100), 67 (41), 57 (38).

Data of ²H-9. ²H-NMR (600 MHz, CDCl₃): 1.26 (br. s, Me₂CD). EI-MS: 181 (2, *M*⁺), 152 (1), 123 (10), 107 (3), 101 (22), 81 (100), 67 (16), 57 (9).

Data of ²H-10. ²H-NMR (600 MHz, CDCl₃): 0.98 (br. s, 0.1 D, (CH₂D)_{endo}–C(4)); 0.69 (br. s, 0.9 D, (CH₂D)_{exo}–C(4)). EI-MS: 181 (2, *M*⁺), 166 (1), 152 (1), 137 (1), 123 (9), 109 (2), 98 (5), 81 (100), 67 (8), 55 (7).

3.4. (2*E*)-1-[(1*R*,3*S*)-1-Methyl-3-(1-methylethyl)cyclopent-1-yl]but-2-en-1-one ((*E*)-**17**). Following *GP 2*, **2** (3.50 g, 18.0 mmol) was thermo-isomerized at 620°. The crude product was purified by CC (hexane/AcOEt 40:1) to give a 1:1 mixture of (*Z*)-**17** and **16** (1.19 g, 37%), followed by pure (*E*)-**17** (0.70 g, 20%) as a colorless oil. It was not possible to obtain pure samples of (*Z*)-**17** or **16**. $[\alpha]_{\text{D}}^{23} = -5.5$ ($c = 1.0$, CH₂Cl₂). IR (film): 3044w, 2958vs, 2870vs, 1692vs, 1629vs, 1445vs, 1384s, 1375s, 1367s, 1315s, 1292s, 1170w, 1124m, 1063s, 1046m, 969vs, 931s,

737m. ¹H-NMR (300 MHz, CDCl₃): 6.96 (dq, ³J_{trans} = 15.2, ³J = 6.9, H-C(3)); 6.41 (dq, ³J_{trans} = 15.2, ⁴J = 1.7, H-C(2)); 2.16 (ddd, J = 12.9, 9.1, 3.7, H_{exo}-C(5')); 1.89 (dd, ³J = 6.9, ⁴J = 1.7, Me(4)); 1.88–1.81 (m, H_{endo}-C(4')); 1.73–1.61 (m, CH₂(2'), H-C(3')); 1.41 (ddd, J = 12.9, 8.7, 3.5, H_{endo}-C(5')); 1.26–1.21 (m, H_{exo}-C(4'), Me₂CH); 1.20 (s, Me-C(1')); 0.890, 0.886 (2d, ³J = 6.6, Me₂CH). ¹³C-NMR (75 MHz, CDCl₃): 203.5 (s, C(1)); 142.4 (d, C(3)); 127.2 (d, C(2)); 54.0 (s, C(1')); 47.0 (d, C(3')); 41.2 (t, C(2')); 35.1 (t, C(5')); 33.6 (d, Me₂CH); 30.7 (t, C(4')); 25.5 (q, Me-C(1')); 21.7, 21.6 (2q, Me₂CH); 18.3 (q, C(4)). EI-MS: 194 (2, M⁺), 179 (2, [M - CH₃]⁺), 151 (4), 123 (7), 111 (6), 81 (21), 69 (100), 55 (16).

3.5. 1-[(1R,3S)-1-Methyl-3-(1-methylethenyl)cyclopent-1-yl]-2-methylpropan-1-one (**19**), 1-[(1R,3S)-1-Methyl-3-(1-methylethyl)cyclopent-1-yl]-2-methylprop-2-en-1-one (**20**), and (1R,5S)-1,3,4-Trimethylbicyclo[3.2.1]oct-3-en-2-one (**21**). Following GP 2, **3** (3.50 g, 18.0 mmol) was thermo-isomerized at 620°. The crude product was purified by CC (hexane/AcOEt 50:1) to give pure **19** (0.49 g, 14%), followed by **20** (0.42 g, 12%) and a mixed fraction (0.10 g) of **20** and two unidentified components in a 2:1:1 ratio (GC analysis), and pure **21** (1.39 g, 7.38 mmol, 47%) as a colorless oil.

Data of **19**. [α]_D²⁵ = -6.1 (c = 1.0, CH₂Cl₂). IR (film): 3076w, 2962vs, 2870s, 1706vs, 1645w, 1452s, 1375m, 1256m, 1080w, 989m, 735m. ¹H-NMR (600 MHz, CDCl₃): 4.72 (br. s, H of isopropenyl); 4.69 (br. s, H of isopropenyl, NOE with Me of isopropenyl); 3.03 (sept., ³J = 6.7, H-C(2)); 2.70–2.59 (m, H-C(3')); 2.22 (ddd, J = 12.8, 8.2, 3.1, H_{exo}-C(5')); 1.94–1.84 (m, H_{exo}-C(2'), H_{endo}-C(4')); 1.73 (s, Me of isopropenyl); 1.71–1.64 (m, H_{endo}-C(2')); 1.50–1.42 (m, H_{exo}-C(4'), H_{endo}-C(5')); 1.27 (s, Me-C(1')); 1.02, 1.00 (2d, ³J = 6.7, Me₂CH). ¹³C-NMR (150 MHz, CDCl₃): 214.7 (s, C(1)); 147.5 (s, C-C(3')); 108.7 (t, CH₂ of isopropenyl); 52.8 (s, C(1')); 45.8 (d, C(3')); 38.6 (t, C(2')); 35.8 (d, Me₂CH); 33.3 (t, C(5')); 30.8 (t, C(4')); 24.7 (q, Me-C(1')); 20.33, 20.27 (2q, Me₂CH); 20.1 (q, Me of isopropenyl). EI-MS: 194 (4, M⁺), 151 (7), 123 (78), 107 (18), 81 (100), 67 (33), 55 (24).

Data of **20**. [α]_D²⁵ = -5.8 (c = 1.0, CH₂Cl₂). IR (film): 3083w, 2964vs, 2872vs, 1668vs, 1470s, 1381s, 1299w, 1261w, 1077m, 1042m, 971m, 886m. ¹H-NMR (600 MHz, CDCl₃): 5.64, 5.60 (2 br. s, CH₂(2)); 2.08 (ddd, J = 12.7, 8.7, 3.5, H_{exo}-C(5')); 1.91 (q, Me-C(2)); 1.83–1.78 (m, H_{endo}-C(4')); 1.71–1.60 (m, CH₂(2'), H-C(3')); 1.44–1.37 (m, H_{endo}-C(5')); 1.25–1.21 (m, H_{exo}-C(4'), Me₂CH); 1.23 (s, Me-C(1')); 0.890, 0.886 (2d, ³J = 6.6, Me₂CH). ¹³C-NMR (150 MHz, CDCl₃): 201.4 (s, C(1)); 146.2 (s, C(2)); 122.0 (t, C(3)); 54.8 (s, C(1')); 47.0 (d, C(3')); 42.8 (t, C(2')); 37.1 (t, C(5')); 33.4 (d, Me₂CH); 30.6 (t, C(4')); 25.4 (q, Me-C(1')); 21.63, 21.61 (2q, Me₂CH); 20.0 (q, Me-C(2')). EI-MS: 194 (8, M⁺), 151 (3), 123 (100), 109 (18), 95 (15), 83 (41), 69 (29), 55 (36).

Data of **21**. [α]_D²⁵ = -110.9 (c = 1.85, CH₂Cl₂). IR (film): 2961vs, 2939vs, 2867s, 1666vs, 1446m, 1377s, 1291w, 1254m, 1163w, 1123w, 1094w, 1028m, 940w, 889w, 735w. ¹H-NMR (300 MHz, CDCl₃): 2.68 (br. t, J = 5.2, H-C(5)); 2.10–2.00 (m, H_{endo}-C(6)); 1.96 (d, J = 0.8, Me-C(4)); 1.80 (br. d, J = 11.4, H_{gem}-C(8)); 1.69 (s, Me-C(3)); 1.68–1.51 (m, H_{exo}-C(6), CH₂(7)); 1.48 (dd, J = 11.4, 4.2, H_{ann}-C(8)); 1.25 (s, Me-C(1)). ¹³C-NMR (75 MHz, CDCl₃): 204.0 (s, C(2)); 160.8 (s, C(4)); 127.5 (s, C(3)); 51.6 (s, C(1)); 46.2 (t, C(8)); 45.2 (d, C(5)); 33.2 (t, C(7)); 29.9 (t, C(6)); 20.5 (q, Me-C(1)); 20.0 (q, Me-C(4)); 10.5 (q, Me-C(3)). EI-MS: 164 (55, M⁺), 149 (8, [M - CH₃]⁺), 135 (21, [M - C₂H₅]⁺), 121 (16), 109 (100), 95 (11), 81 (56), 79 (34), 65 (9), 53 (19). HR-EI-MS: 164.1200 (M⁺, C₁₁H₁₆O⁺; calc. 164.1201).

3.6. 1-[(1R,3S)-1-Methyl-3-(1-methylethenyl)cyclopent-1-yl]-2-methyl[2-²H]propan-1-one ([²H]-**19**), 1-[(1R,3S)-3-(1-Methyl[1-²H]ethyl)-1-methylcyclopent-1-yl]-2-methylprop-2-en-1-one ([²H]-**20**), and (1R,5S)-4-(²H[Methyl]-1,3-dimethylbicyclo[3.2.1]oct-3-en-2-one ([²H]-**21**). Following GP 2, [²H]-**3** (1.25 g, 6.40 mmol) was thermo-isomerized at 620°. Purification as described for unlabeled **3** afforded pure samples of each compound.

Data of [²H]-**19**. ²H-NMR (600 MHz, CDCl₃): 3.08–3.00 (m, D-C(2)). EI-MS: 195 (4, M⁺), 151 (7), 124 (33), 123 (56), 107 (20), 81 (100), 67 (35), 55 (29).

Data of [²H]-**20**. ²H-NMR (600 MHz, CDCl₃): 1.24 (br. s, Me₂C). EI-MS: 195 (3, M⁺), 151 (14), 124 (100), 123 (21), 107 (25), 96 (16), 84 (35), 55 (32).

Data of [²H]-**21**. ²H-NMR (600 MHz, CDCl₃): 1.96 (br. s, DH₂C-C(4)). EI-MS: 165 (36, M⁺), 149 (8, [M - CH₃D]⁺), 136 (33, [M - C₂H₅]⁺), 121 (16), 109 (100), 93 (6), 82 (44), 81 (51), 79 (34), 65 (9), 53 (31).

3.7. 1-[(1R,3S)-1-Methyl-3-(1-methylethenyl)cyclopent-1-yl]prop-2-en-1-one (**24**) and (1R,5S)-3-Ethyl-1,4-dimethylbicyclo[3.2.1]oct-3-en-2-one (**25**). Following GP 2, **6** (2.81 g, 15.8 mmol) was thermo-isomerized at 620°. The crude product was purified by CC (hexane/AcOEt 40:1) to give **24** (1.38 g, 49%) and **25** (0.42 g, 15%) as colorless oils.

Data of **24**. [α]_D²⁵ = -6.6 (c = 1.0, CH₂Cl₂). IR (film): 3074w, 3021w, 2962vs, 2870s, 1695vs, 1645s, 1611s, 1456s, 1400vs, 1376m, 1296w, 1268w, 1218w, 1200w, 1147w, 1057m, 1029m, 986s, 888s, 795w, 737w. ¹H-NMR (500 MHz, CDCl₃): 6.70 (dd, ³J_{trans} = 17.0, ³J_{cis} = 10.4, H-C(2)); 6.38 (dd, ³J_{trans} = 17.0, ²J = 2.0, H_{trans}-C(3)); 5.68

(*dd*, $^3J_{cis} = 10.4$, $^2J = 2.0$, $H_{cis} - C(3)$); 4.72 (br. *s*, H of isopropenyl); 4.70 (br. *s*, H of isopropenyl, NOE with Me of isopropenyl); 2.69–2.64 (*m*, H–C(3')); 2.26 (*ddd*, $J = 12.0$, 8.9, 3.7, $H_{exo} - C(5')$); 1.97–1.84 (*m*, $H_{exo} - C(2')$, $H_{endo} - C(4')$); 1.73 (*s*, Me of isopropenyl); 1.67 (*ddd*, $J = 12.9$, 6.9, 1.3, $H_{endo} - C(2')$); 1.51–1.47 (*m*, $H_{exo} - C(4')$, $H_{endo} - C(5')$); 1.26 (*s*, Me–C(1')). ^{13}C -NMR (125 MHz, $CDCl_3$): 202.7 (*s*, C(1)); 147.3 (*s*, C–C(3')); 131.8 (*d*, C(2)); 128.3 (*t*, C(3)); 109.9 (*t*, CH_2 of isopropenyl); 53.6 (*s*, C(1')); 46.0 (*d*, C(3')); 40.8 (*t*, C(2')); 35.3 (*t*, C(5')); 31.0 (*t*, C(4')); 25.3 (*q*, Me–C(1')); 20.2 (*q*, Me of isopropenyl). EI-MS: 178 (3, M^{+}), 163 (3, $[M - CH_3]^+$), 135 (2), 123 (62), 107 (12), 95 (15), 81 (100), 67 (36), 55 (71).

Data of 25. $[\alpha]_D^{25} = -106.2$ ($c = 1.0$, CH_2Cl_2). IR (film): 2961vs, 2940vs, 2868vs, 1666vs, 1447vs, 1379vs, 1293m, 1242s, 1161w, 1123m, 1105m, 1065w, 1045s, 927w, 900w, 885m, 829m, 735w. 1H -NMR (500 MHz, $CDCl_3$): 2.66 (br. *t*, $J = 5.1$, H–C(5)); 2.22 (*A* of ABX_3 , $J_{AB} = 15.0$, $J_{AX} = 7.5$, H_a of CH_2Me); 2.20 (*B* of ABX_3 , $J_{AB} = 15.0$, $J_{BX} = 7.5$, H_b of CH_2Me); 2.11–2.01 (*m*, $H_{endo} - C(6)$); 1.96 (*s*, Me–C(4)); 1.79 (br. *d*, $J = 11.2$, $H_{syn} - C(8)$); 1.71–1.51 (*m*, $H_{exo} - C(6)$, $CH_2(7)$); 1.48 (*dd*, $J = 11.2$, 4.2, $H_{anti} - C(8)$); 1.24 (*s*, Me–C(1)); 0.87 (*t*, $^3J = 7.5$, CH_2Me). ^{13}C -NMR (125 MHz, $CDCl_3$): 203.4 (*s*, C(2)); 160.3 (*s*, C(4)); 133.6 (*s*, C(3)); 51.6 (*s*, C(1)); 46.1 (*t*, C(8)); 45.1 (*d*, C(5)); 33.2 (*t*, C(7)); 30.0 (*t*, C(6)); 20.4 (*q*, Me–C(1)); 19.5 (*q*, Me–C(4)); 18.0 (*t*, CH_2Me); 13.2 (*q*, CH_2Me). EI-MS: 178 (53, M^{+}), 163 (10, $[M - CH_3]^+$), 149 (22, $[M - C_2H_5]^+$), 135 (22), 122 (80), 107 (12), 95 (100), 79 (24), 67 (27), 55 (21). HR-EI-MS: 178.1355 (M^+ ; $C_{12}H_{18}O^+$; calc. 178.1358).

3.8. *1-[(1R,3S)-1-Methyl-3-(1-methylethenyl)cyclopent-1-yl][2- 2H]prop-2-en-1-one* ($[2-^2H]$ -**24**), (*1R,5S*)-3- $[(2-^2H)Ethyl]$ -1,4-dimethylbicyclo[3.2.1]oct-3-en-2-one ($[2-^2H]$ -**25**), and (*1R,5S*)-3-Ethyl-4-(2H -methyl)-1-methylbicyclo[3.2.1]oct-3-en-2-one ($[3-^2H]$ -**25**). Following GP 2, $[O-^2H]$ -**6** (0.69 g, 3.85 mmol) was thermo-isomerized at 620°. Purification as described for unlabeled **6** afforded $[2-^2H]$ -**24** and a 1:1 mixture of $[2-^2H]$ -**25** and $[3-^2H]$ -**25**.

Data of $[2-^2H]$ -24. 2H -NMR (600 MHz, $CDCl_3$): 6.71 (br. *s*, D–C(2)). EI-MS: 179 (2, M^{+}), 164 (5, $[M - CH_3]^+$), 135 (9), 123 (40), 107 (11), 95 (14), 81 (100), 67 (36), 55 (46).

Data of $[2-^2H]$ - and $[3-^2H]$ -25. 2H -NMR (600 MHz, $CDCl_3$): 1.96 (br. *t*, $J = 7.4$, $DH_2C - C(4)$); 0.87 (br. *t*, $J = 7.5$, DCH_2CH_2). EI-MS: 179 (50, M^{+}), 164 (10, $[M - CH_3]^+$), 163 (8, $[M - CH_2D]^+$), 149 (18, $[M - C_2H_4D]^+$), 148 (13, $[M - C_2H_5]^+$).

3.9. (*E/Z*)-1- $[(1R,3S)$ -1-Methyl-3-(1-methylethenyl)cyclopent-1-yl][3- 2H]prop-2-en-1-one ((*E*)/(*Z*)- $[3-^2H]$ -**24**) and (*1R,5S*)-3- $[(1-^2H)Ethyl]$ -1,4-dimethylbicyclo[3.2.1]oct-3-en-2-one ($[1-^2H]$ -**25**). Following GP 2, $[2-^2H]$ -**6** (1.23 g, 6.86 mmol) was thermo-isomerized at 620°. Purification as described for unlabeled **6** afforded a 1:1 mixture of (*E/Z*)- $[3-^2H]$ -**24**, and pure $[1-^2H]$ -**25**.

Data of (*E/Z*)- $[3-^2H]$ -24. 2H -NMR (600 MHz, $CDCl_3$): 6.39 (br. *d*, $J \approx 15$, $D_{trans} - C(3)$); 5.69 (br. *d*, $J \approx 9$, $D_{cis} - C(3)$). EI-MS: 179 (2, M^{+}), 164 (3, $[M - CH_3]^+$), 136 (2), 123 (44), 107 (12), 95 (13), 81 (100), 67 (43), 55 (49).

Data of $[1-^2H]$ -25. 2H -NMR (600 MHz, $CDCl_3$): 2.39–2.05 (*m*, $CHDMe$). EI-MS: 179 (50, M^{+}), 164 (10, $[M - CH_3]^+$), 149 (18, $[M - C_2H_4D]^+$), 136 (21), 123 (75), 108 (12), 96 (100), 79 (19), 68 (20), 55 (21).

3.10. *1-[(1R,3S)-1-Methyl-3-(1-methylethenyl)cyclopent-1-yl][2,3- $^{13}C_2$]prop-2-en-1-one* ($[^{13}C_2]$ -**24**) and (*1R,5S*)-3- $[(1-^{13}C)Ethyl]$ -1,4-dimethylbicyclo[3.2.1]oct-3-en-2-one ($[^{13}C_2]$ -**25**). Following GP 2, $[^{13}C_2]$ -**6** (2.81 g, 15.8 mmol) was thermo-isomerized at 620°. Purification as described for unlabeled **6** afforded pure samples of either compound.

Data of $[^{13}C_2]$ -24. ^{13}C -NMR (75 MHz, $CDCl_3$): 131.8 (*d*, $^2J(C,C) = 68.2$, C(2)); 128.3 (*d*, $^2J(C,C) = 68.2$, C(3)). EI-MS: 180 (2, M^{+}), 165 (2, $[M - CH_3]^+$), 151 (1), 147 (1), 137 (2), 123 (44), 107 (9), 95 (6), 93 (4), 81 (100), 67 (38), 57 (29), 55 (32).

Data of $[^{13}C_2]$ -25. ^{13}C -NMR (75 MHz, $CDCl_3$): 133.6 (*d*, $^2J(C,C) = 45.5$, C(3)); 18.0 (*d*, $^2J(C,C) = 45.5$, $MeCH_2$). EI-MS: 180 (43, M^{+}), 165 (8, $[M - CH_3]^+$), 152 (8), 150 (7), 137 (22), 124 (75), 123 (59), 109 (9), 97 (100), 93 (10), 81 (13), 79 (12), 69 (43), 55 (49).

3.11. *1-[(1R,3S)-1-Methyl-3-(1-methylethyl)cyclopent-1-yl](phenyl)methanone* (**26**). Following GP 2, **7** (1.38 g, 5.99 mmol) was thermo-isomerized at 630°. The yellow crude product was purified by CC (hexane/AcOEt 30:1) to give **26** (0.66 g, 48%) as a pale yellow oil, which was further distilled (*Kugelrohr*), affording a colorless liquid. $[\alpha]_D^{25} = -6.7$ ($c = 1.0$, hexane). IR (film): 3060w, 2957vs, 2871vs, 1674vs, 1598s, 1579s, 1447vs, 1384m, 1367m, 1284s, 1236s, 1184s, 1159s, 1077w, 1003m, 975s, 942m, 797m, 714vs, 656w. 1H -NMR (600 MHz, $CDCl_3$): 7.86 (*dd*, $^3J = 7.2$, $^4J = 1.4$, 2 H_o of Ph); 7.47 (*tt*, $^3J = 7.4$, $^4J = 1.2$, H_p of Ph); 7.41 (*t*, $^3J = 7.5$, 2 H_m of Ph); 2.45 (*ddd*, $J = 13.2$, 9.4, 3.7, $H_{exo} - C(5')$); 1.91–1.86 (*m*, $CH_2(2)$, $H_{endo} - C(4')$); 1.75 (*sext.*, $J = 7.9$, H–C(3')); 1.66 (*ddd*, $J = 13.2$, 8.7, 3.6, $H_{endo} - C(5')$); 1.42 (*s*, Me–C(1')); 1.38 (*sext.* \times *d*, $J = 6.7$, 1.7, Me_2CH); 1.30–1.23 (*m*, $H_{exo} - C(4')$); 0.90, 0.89 (*2d*, $J = 6.7$, Me_2CH). ^{13}C -NMR (150 MHz, $CDCl_3$): 206.7 (*s*, C(1)); 136.9 (*s*, C_{ipso} of Ph); 131.8 (*d*, C_p of Ph); 129.2 (*d*, C_o of Ph); 128.3 (*d*, C_m of Ph); 54.7 (*s*, C(1')); 46.9 (*d*, C(3')); 43.2 (*t*, C(2')); 37.6 (*t*, C(5')); 33.6 (*d*, Me_2CH); 30.6 (*t*, C(4')); 28.0 (*q*, Me–C(1')); 21.8, 21.7 (*2q*, Me_2CH). EI-MS: 230

(4, M^{++}), 212 (1, $[M - H_2O]^{++}$), 187 (10), 124 (25, $[M - C(=O)Ph]^{++}$), 105 (100, $COPh^+$), 81 (63), 69 (80), 55 (28). Anal. calc. for $C_{16}H_{22}O$ (230.35): C 83.43, H 9.63; found: C 83.39, H 9.66.

3.12. *[(1R,3S)-3-(1-Methyl[1- 2 H]ethyl)-1-methylcyclopent-1-yl](phenyl)methanone* ($[^2H]$ -**26**). Following GP 2, $[O-^2H]$ -**7** (0.88 g, 3.10 mmol) was thermo-isomerized at 630°. Purification as described for unlabeled **26** afforded pure $[^2H]$ -**26**. 2H -NMR (300 MHz, $CDCl_3$): 1.38 (br. s, Me_2CD). EI-MS: 231 (5, M^{++}), 213 (1, $[M - H_2O]^{++}$), 188 (12), 125 (22, $[M - C(=O)Ph]^{++}$), 105 (100, $COPh^+$), 81 (58), 69 (72), 55 (23).

4. *Derivatization of DGPTI Products*. 4.1. *(1R,5S)-1,3,3,4,4-Pentamethylbicyclo[3.2.1]octan-2-one* (**22**). To a soln. of LDA, freshly prepared by addition of a 2.4M soln. of BuLi in hexane (3.46 ml, 8.32 mmol) to i -Pr $_2$ NH (1.38 ml, 9.71 mmol) in THF (15 ml) at -78° , was added **10** (0.50 g, 2.77 mmol) in THF (4 ml) at -78° . After stirring at that temperature for 0.5 h, the soln. was warmed to r.t. and stirred for an additional 0.5 h. After recooling to -78° , MeI (1.38 ml, 22.16 mmol) was added, the mixture was allowed to warm to r.t., and stirring was continued overnight. The reaction was quenched with a sat. soln. of NH_4Cl (20 ml). The mixture was poured into a separatory funnel containing Et $_2$ O (30 ml). The org. layer was separated, and the aq. phase was extracted with Et $_2$ O (3 \times 20 ml). The combined org. layers were washed with brine, dried ($MgSO_4$), filtered, and concentrated *in vacuo* to afford **22** (0.511 g, 95%) as a yellow oil. $[\alpha]_D^{25} = -59.6$ ($c = 0.76$, CH_2Cl_2). IR (film): 2965vs, 2931vs, 2871s, 1699vs, 1645w, 1482m, 1460s, 1395m, 1377m, 1291w, 1127w, 1082m, 1011s, 954m, 885m. 1H -NMR (600 MHz, $CDCl_3$): 2.22 (dddd, $J = 16.0, 9.2, 4.9, 2.4$, $H_{endo}-C(6)$); 1.96–1.93 (m , $H_{syn}-C(8)$); 1.93–1.84 (m , $H-C(5)$, $H_{exo}-C(6)$, $H_{endo}-C(7)$); 1.59–1.55 (m , $H_{exo}-C(7)$); 1.55 (dd , $J = 12.3, 4.5$, $H_{anti}-C(8)$); 1.13 (s , $Me-C(1)$); 1.12 (s , $Me_{endo}-C(3)$); 0.99 (s , $Me_{endo}-C(4)$); 0.95 (s , $Me_{exo}-C(3)$); 0.91 (s , $Me_{exo}-C(4)$). ^{13}C -NMR (150 MHz, $CDCl_3$): 219.8 (s , $C(2)$); 52.7 (s , $C(1)$); 50.1 (s , $C(3)$); 50.0 (d , $C(5)$); 40.9 (t , $C(8)$); 40.5 (s , $C(4)$); 35.3 (t , $C(7)$); 28.7 (q , $Me_{exo}-C(4)$); 27.9 (q , $Me_{endo}-C(3)$); 25.5 (t , $C(6)$); 23.4 (q , $Me_{exo}-C(3)$); 23.2 (q , $Me_{endo}-C(4)$); 21.3 (q , $Me-C(1)$). EI-MS: 194 (5, M^{++}), 179 (3), 165 (1), 151 (4), 138 (2), 122 (7), 111 (7), 95 (5), 81 (100), 69 (23), 55 (14).

4.2. *[(1R,3S)-1-Methyl-3-(1-methylethyl)cyclopent-1-yl] Benzoate* (**28**). Phenone **26** (0.29 g, 1.26 mmol) was dissolved in anhyd. CH_2Cl_2 (6 ml), and m -MCPBA (80–85%; 0.57 g, 3.27 mmol) was added. The suspension was cooled to 0° , and TFA (96 μ l, 1.26 mmol) was added dropwise. The mixture was stirred at r.t. for 20 d in the dark. The mixture was diluted with CH_2Cl_2 (50 ml), and washed once each with 10% aq. Na_2SO_3 soln., sat. aq. K_2CO_3 soln., and H_2O . The org. phase was dried ($MgSO_4$), and evaporated. The residue was taken up in hexane and filtered over a short pad of SiO_2 using hexane/AcOEt 50 : 1 to give **28** (0.28 g, 89%) as a colorless oil. $[\alpha]_D^{25} = -6.2$ ($c = 1.0$, CH_2Cl_2). IR (film): 3063w, 3033w, 2961vs, 2871vs, 1714vs, 1602m, 1584m, 1451s, 1375s, 1292vs, 1315vs, 1176s, 1115vs, 1070s, 1026s, 854w, 713vs. 1H -NMR (600 MHz, $CDCl_3$): 7.99 (A of $AA'BB'C$, 2 H_o of Ph); 7.52 (C of $AA'BB'C$, H_p of Ph); 7.41 (B of $AA'BB'C$, 2 H_m of Ph); 2.31 (m , $H_{endo}-C(5')$); 2.18 (A of ABX , $^2J_{AB} = 13.6$, $^3J(2',3') = 8.0$, $H_{endo}-C(2')$); 1.89 (B of ABX , $^2J_{AB} = 13.6$, $^3J(2'_{exo},3') = 9.9$, $H_{exo}-C(2')$); 1.82–1.76 (m , $H_{endo}-C(4')$, $H_{exo}-C(5')$); 1.67–1.62 (m , $H-C(3')$); 1.66 (s , $Me-C(1')$); 1.49–1.41 (m , 2 $H_{exo}-C(4')$, Me_2CH); 0.90, 0.89 ($2d$, $J = 6.4, 5.9$, Me_2CH). ^{13}C -NMR (150 MHz, $CDCl_3$): 165.8 (s , $C(1)$); 132.6 (d , C_p of Ph); 132.1 (s , C_{ipso} of Ph); 129.6 (d , C_o of Ph); 128.4 (d , C_m of Ph); 90.1 (s , $C(1')$); 46.3 (d , $C(3')$); 44.4 (t , $C(2')$); 39.8 (t , $C(5')$); 33.9 (d , Me_2CH); 29.2 (t , $C(4')$); 25.6 (q , $Me-C(1')$); 21.6, 21.4 ($2q$, Me_2CH). EI-MS: 246 (1, M^{++}), 124 (27, $[M - CO_2Ph]^{++}$), 105 (100), 81 (54), 69 (7), 55 (3).

4.3. *(1R,3S)-1-Methyl-3-(1-methylethyl)cyclopentan-1-ol* (**29**). To a stirred soln. of **28** (0.22 g, 0.89 mmol) in MeOH (2 ml) was added at 0° a sat. aq. LiOH soln. (2 ml). The mixture became immediately dark and cloudy. After stirring overnight at r.t., 2N NaOH soln. (2 ml) was added, and the mixture was extracted with Et $_2$ O (3 \times). The combined org. layers were washed with brine, dried ($MgSO_4$), and evaporated to afford **29** (0.11 g, 90%) as a colorless solid. M.p. 70–72°. $[\alpha]_D^{25} = -4.0$ ($c = 1.0$, CH_2Cl_2). IR ($CHCl_3$): 3692m, 3608m, 2961vs, 2873vs, 1603s, 1471m, 1385w, 1368m, 1316w, 1262m, 1104s, 1023m. 1H -NMR (600 MHz, $CDCl_3$): 1.86 (dd , $^2J = 13.2$, $^3J = 8.5$, $H_{endo}-C(2)$); 1.78–1.72 (m , $H_{endo}-C(4)$); 1.71 (ddd , $J = 11.5, 7.9, 3.0$, $H_{endo}-C(5)$); 1.62–1.54 (m , $H-C(3)$, $H_{exo}-C(5)$); 1.50–1.43 (m , $H_{exo}-C(4)$, Me_2CH); 1.42 (s , OH); 1.40 (dd , $^2J = 13.2$, $^3J = 9.3$, $H_{exo}-C(2)$); 1.33 (s , $Me-C(1')$); 0.89, 0.87 ($2q$, $J = 6.5$, Me_2CH). ^{13}C -NMR (150 MHz, $CDCl_3$): 76.4 (s , $C(1)$); 47.0 (d , $C(3)$); 46.6 (t , $C(2)$); 42.0 (t , $C(5)$); 34.2 (d , Me_2CH); 29.7 (t , $C(4)$); 29.4 (q , $Me-C(1)$); 21.7, 21.4 ($2q$, Me_2CH). EI-MS: 142 (1, M^{++}), 124 (27, $[M - H_2O]^{++}$), 109 (43), 99 (78), 84 (54), 71 (100), 55 (50).

REFERENCES

- [1] K. Alder, F. Pascher, A. Schmitz, *Ber. Dtsch. Chem. Ges.* **1943**, 76, 27.
 [2] H. M. R. Hoffmann, *Angew. Chem., Int. Ed.* **1969**, 8, 556.

- [3] G. V. Boyd, in 'The Chemistry of Double-Bonded Functional Groups', Ed. S. Patai, J. Wiley & Sons, New York, 1989, Vol. 2, Suppl. A, Part 1, p. 477.
- [4] B. B. Snider, in 'Comprehensive Organic Synthesis', Ed. B. M. Trost, I. Fleming, Pergamon Press, London, 1991, Vol. V.1, p. 1.
- [5] B. B. Snider, D. J. Rodini, J. van Straten, *J. Am. Chem. Soc.* **1980**, *102*, 5872.
- [6] D. F. Taber, 'Intramolecular Diels–Alder and Alder–Ene Reactions', Springer, Berlin, 1984, p. 61.
- [7] W. Oppolzer, V. Snieckus, *Angew. Chem., Int. Ed.* **1978**, *17*, 476.
- [8] J.-L. Ripoll, Y. Vallée, *Synthesis* **1993**, 659.
- [9] J. M. Conia, P. Le Perche, *Synthesis* **1975**, 1.
- [10] S. A. Monti, T. W. McAninch, *Tetrahedron Lett.* **1974**, *15*, 3239.
- [11] V. Dimitrov, S. Bratovanov, S. Simova, K. Kostova, *Tetrahedron Lett.* **1994**, *35*, 6713.
- [12] F. Näf, P. Degen, *Helv. Chim. Acta* **1971**, *54*, 1939.
- [13] P. Gosselin, D. Joulain, P. Laurin, R. F. *Tetrahedron Lett.* **1990**, *31*, 3151.
- [14] D. S. Keegan, M. M. Midland, R. T. Werley, J. I. McLoughlin, *J. Org. Chem.* **1991**, *56*, 1185.
- [15] V. I. Potkin, E. A. Dikusar, N. G. Kozlov, *Russ. J. Org. Chem.* **2002**, *38*, 1260.
- [16] D. F. Taber, P. H. Storck, *J. Org. Chem.* **2002**, *67*, 8273.
- [17] V. Lecompte, E. Stéphane, G. Jaouen, *Tetrahedron Lett.* **2001**, *42*, 5409.
- [18] V. Lecompte, E. Stéphane, G. Jaouen, *Tetrahedron Lett.* **2002**, *43*, 3463.
- [19] J. M. Coxon, P. J. Steel, *Aust. J. Chem.* **1979**, *32*, 2441.
- [20] R. F. C. Brown, 'Pyrolytic Methods in Organic Chemistry: Application of Flow and Flash Vacuum Pyrolytic Techniques', Academic Press, New York, 1980.
- [21] H. McNab, *Contemp. Org. Synth.* **1996**, *3*, 373.
- [22] M. Nagel, G. Fräter, H.-J. Hansen, *Chimia* **2003**, *57*, 196.
- [23] G. Rüedi, M. Nagel, H.-J. Hansen, *Org. Lett.* **2003**, *5*, 2691.
- [24] G. Rüedi, H.-J. Hansen, *Helv. Chim. Acta* **2004**, *87*, 1968.
- [25] G. Rüedi, M. Nagel, H.-J. Hansen, *Synlett* **2003**, 1210.
- [26] L. A. Paquette, J. F. P. Andrews, C. Vanucci, D. E. Lawhorn, J. T. Negri, R. D. Rogers, *J. Org. Chem.* **1992**, *57*, 3956.
- [27] H. Meerwein, W. Unkel, *Justus Liebigs Ann. Chem.* **1910**, *376*, 152.
- [28] J. P. Perdew, K. Burke, M. Ernzerhof, *Phys. Res. Lett.* **1996**, *77*, 3865.
- [29] D. N. Laikov, *Chem. Phys. Lett.* **1997**, *281*, 151.
- [30] J. Bredt, H. Thouet, J. Schmitz, *Liebigs Ann. Chem.* **1924**, *437*, 1.
- [31] W. Grimme, M. W. Harter, C. A. Sklorz, *J. Chem. Soc., Perkin Trans. 2* **1999**, 1959.
- [32] K. W. Egger, D. M. Golden, S. W. Benson, *J. Am. Chem. Soc.* **1964**, *86*, 5420.
- [33] K. W. Egger, A. T. Cooks, *Helv. Chim. Acta* **1973**, *56*, 1516.
- [34] K. W. Egger, A. T. Cooks, *Helv. Chim. Acta* **1973**, *56*, 1537.
- [35] M. T. M. Clements, R. E. Klinck, S. Peiris, A. J. Ragauskas, J. B. Stothers, *Can. J. Chem.* **1988**, *66*, 454.
- [36] V. Grignard, F. Chambret, *C. R. Acad. Sci.* **1926**, *182*, 299.
- [37] R. L. Failes, V. R. Stimson, in 'The Chemistry of the Hydroxy Group', Ed. S. Patai, J. Wiley & Sons, Chichester, 1980, p. 449.
- [38] J. L. Holmes, F. P. Lossing, *J. Am. Chem. Soc.* **1982**, *104*, 2648.
- [39] G. Chuchani, A. Rotinov, R. Dominguez, *Int. J. Chem. Kinet.* **1999**, *31*, 401.
- [40] J. A. Berson, *Acc. Chem. Res.* **1968**, *1*, 152.
- [41] R. B. Woodward, R. Hoffmann, *J. Am. Chem. Soc.* **1965**, *87*, 2511.
- [42] R. Hoffmann, R. B. Woodward, *Acc. Chem. Res.* **1968**, *1*, 17.
- [43] N. G. Ahn, 'Die Woodward-Hoffman-Regeln und ihre Anwendung', Verlag Chemie, Weinheim, 1972.
- [44] F. H. Allen, *Acta Crystallogr., Sect. B* **2002**, *52*, 380.
- [45] S. S. C. Koch, A. R. Chamberlin, *Synth. Commun.* **1989**, *19*, 829.
- [46] F.-Y. Zhang, E. J. Corey, *Org. Lett.* **2000**, *2*, 1097.
- [47] O. Wallach, K. Oldenberg, *Justus Liebigs Ann. Chem.* **1911**, 204.
- [48] O. Wallach, J. Challenger, *Justus Liebigs Ann. Chem.* **1912**, 61.
- [49] G. Rüedi, H.-J. Hansen, *Helv. Chim. Acta* **2004**, *87*, 1638.

Received February 13, 2004